

# A paradox of non-monotonicity in stability of pipes conveying fluid

I. Elishakoff      P. Vittori \*

## Abstract

The paradoxical result of the non-monotonous relationship between the critical speed of the fluid that is conveyed in the elastic pipe, and the mass ratio was reported first some four decades ago. Since then this result was reproduced in numerous books and articles. In this study the paradox is revisited. It appears that it is a numerical artifact; instead of non-monotonicity there are jumps.

## 1 Introduction

Scientists have studied the dynamics of pipes conveying fluid since 1878, when Aitken [1] conducted a series of experiments on traveling chains and elastic cords. In 1939, Bourrieres [6] published the first theoretical study and derived the governing equations of motion. Further researchers derived everything from scratch, being unaware of the existence of Bourrieres work. This was the case with Long [24] and Niordson [27] who investigated the vibration of systems under various boundary conditions; Long was the first one who was specifically interested in cantilever pipes.

In 1961 Benjamin [3][4] was the first to comprehensively report on this phenomenon. He produced a complete theory, supported with experiments for articulated pipe systems. In his work he derived the equation for a chain of articulated pipes based on Lagrangian equations.

---

\*Department of Mechanical Engineering Florida Atlantic University, Boca Raton, FL 33431-0991

Later on, in 1966, Gregory & Païdoussis [17][18] were the first ones to solve the equations of motion by the exact and the approximate methods, as well as introducing the first critical fluid velocity stability plot for cantilever beam, which is shown in Fig.1.

Their pioneering analysis was followed by many other many scientists namely by, R. D. Blevins [5], Chen [7], M. P. Païdoussis & G. X. Li [31], and M. P. Païdoussis [32], all of them reporting *non-monotonic* results for the critical velocity as a function of a non-dimensional parameter  $\beta$ . Please refer to dotted regions 1, 2, and 3 in Fig.1. The dotted lines do not appear in the paper by Gregory & Païdoussis (1966); these are introduced here to identify the regions of non-monotonic behavior.

Based on previous analyses in other fields of stability theory one of the authors was concerned with accuracy of these results. He had a feeling that Fig.1 was not totally correct, basing his comments on the following simple reasoning: “From a linear differential equation of motion one ought to expect to get results of monotonic critical flow velocities for each non-dimensional parameter  $\beta$ . Why should there be three critical velocities for  $\beta$  in vicinity of 0.3, or in vicinity of  $\beta = 0.7$  or in vicinity of  $\beta = 0.9$ ? Why should there be such paradoxical results? Is the paradox of non-monotonicity a numerical artifact?” The results of the study of this contradiction follow.

## 2 Problem formulation

The governing differential equation of the pipe conveying fluid, reads:

$$EI \frac{\partial^4 w}{\partial x^4} + MU^2 \frac{\partial^2 w}{\partial x^2} + 2MU \frac{\partial^2 w}{\partial t \partial x} + (M+m) \frac{\partial^2 w}{\partial t^2} = 0 \quad (1)$$

where  $w(x, t)$  is the pipe's displacement,  $EI$  is the flexural rigidity,  $M$  is the mass fluid per unit length,  $U$  is the flow velocity,  $m$  the pipe mass per unit length,  $x$  the axial coordinate, and  $t$  represents the time. We are seeking a solution in the form

$$w(x, t) = e^{\Omega t} Y(x) \quad (2)$$

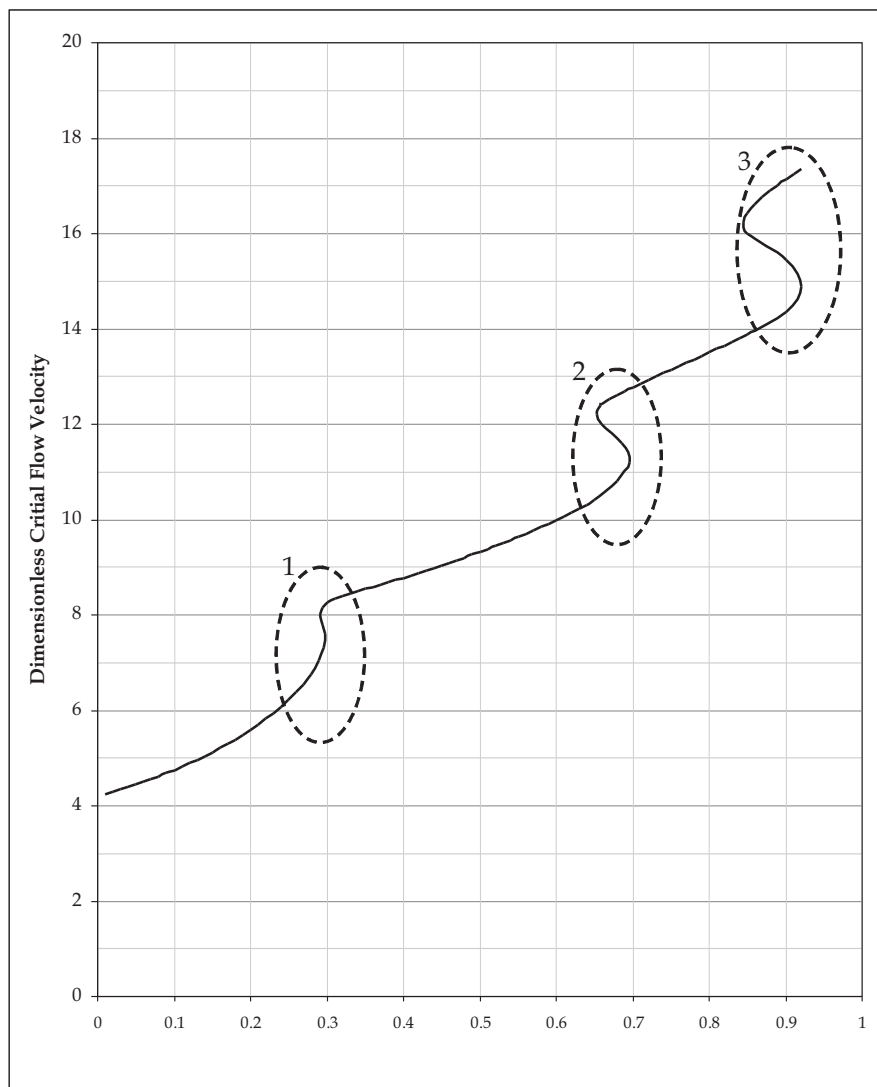


Figure 1: Critical flow velocities according to Gregory & Païdoussis (1966)

Eq.(1) takes the following form

$$EI \frac{d^4 Y(x)}{dx^4} + MU^2 \frac{d^2 Y(x)}{dx^2} + 2MU\Omega \frac{dY(x)}{dx} + (M+m)\Omega^2 Y(x) = 0 \quad (3)$$

Introducing dimensionless axial coordinate  $\xi = x/L$ , and dividing each term by coefficient in the first term  $EI/L^4$ , we obtain

$$\frac{d^4 Y(\xi)}{d\xi^4} + \frac{MU^2 L^2}{EI} \frac{d^2 Y(\xi)}{d\xi^2} + \frac{2L^3 MU\Omega}{EI} \frac{dY(\xi)}{d\xi} + \frac{L^4(M+m)}{EI} \Omega^2 Y(\xi) = 0 \quad (4)$$

The following dimensionless parameters are also introduced:

$$u = UL \sqrt{\frac{M}{EI}}; \quad \omega = \Omega L^2 \sqrt{\frac{M+m}{EI}}; \quad \beta = \frac{M}{M+m} \quad (5)$$

where  $u$  is the dimensionless fluid velocity

$$\frac{d^4 Y(\xi)}{d\xi^4} + u^2 \frac{d^2 Y(\xi)}{d\xi^2} + 2\sqrt{\beta} u \omega \frac{dY(\xi)}{d\xi} + \omega^2 Y(\xi) = 0 \quad (6)$$

The dimensionless governing differential equation becomes

## 2.1 Approximate solution via Boobnov-Galerkin method

According to Eq.(2), the approximate solution can be written as follows

$$w(\xi, t) = e^{\Omega t} Y(\xi), \quad Y(\xi) = \sum_{r=1}^{\infty} a_r \phi_r(\xi) \quad (7)$$

Based on the universal method of approximate nature developed by Boobnov (1913) and Galerkin (1915), an approximate solution to the differential equation can be found as follows: First the Eq.(7) is rewritten in the following form

$$\mathcal{L}(Y(\xi)) = 0 \quad (8)$$

where  $\mathfrak{L}$  is the differential operator. For this particular case  $\mathfrak{L}$  reads:

$$\mathfrak{L} = \frac{d^4}{d\xi^4} + u^2 \frac{d^2}{d\xi^2} + 2\sqrt{\beta}u\omega \frac{d}{d\xi} + \omega^2 \quad (9)$$

However the number of coordinate functions taken into account cannot be infinite during the numerical implementation. Therefore, Eq.(7) must be replaced by

$$Y_N(\xi) = \sum_{r=1}^N a_r \phi_r(\xi) \quad (r = 1, 2, \dots, N) \quad (10)$$

where  $N$  denotes the number of retained terms. If expression (10) happens to satisfy not only the boundary conditions but also the differential equation (6), it means that the exact solution has been found and the problem is solved. In overwhelming majority of cases this is not the case and the result of replacing equation (10) into (8) does not vanish identically, yielding an error denoted by  $\varepsilon$ :

$$\mathfrak{L}(Y_N(\xi)) = \mathfrak{L}\left(\sum_{r=1}^N a_r \phi_r(\xi)\right) \equiv \varepsilon \quad (11)$$

According to the Boobnov-Galerkin procedure, each coordinate function should be multiplied by this error and also demand orthogonality between each function.

### 3 Beam functions as coordinate functions

Coordinate functions  $\phi_r(\xi)$  must be chosen upon satisfying all the boundary conditions. For a cantilever beam the so-called beam functions are used. They are assigned with free vibrations of the beam without a fluid (Timoshenko, Weaver)

$$\begin{cases} \phi_r(\xi) = \cosh(\lambda_r \xi) - \cos(\lambda_r \xi) - \sigma_r (\sinh(\lambda_r \xi) - \sin(\lambda_r \xi)) \\ \sigma_r = \frac{\sinh(\lambda_r) - \sin(\lambda_r)}{\cosh(\lambda_r) + \cos(\lambda_r)} \end{cases} \quad (12)$$

where  $\lambda_r$  are the corresponding eigenvalues for the cantilever beam, obtainable from the following transcendental equation

$$\cos(\lambda_r) \cosh(\lambda_r) = -1 \quad (13)$$

A complete derivation of previous equation, as well as natural frequencies and mode shapes for a cantilever beam, is given in the Appendix, for the convenience of the reader.

Based on the operator  $\mathfrak{L}$  in Eq.(9), the expression for the error in Eq (11) reads:

$$\begin{aligned} \varepsilon(\xi) &= \sum_{r=1}^N a_r \phi_r^{IV}(\xi) + u^2 \sum_{r=1}^N a_r \phi_r^{II}(\xi) \\ &\quad + 2\sqrt{\beta}u\omega \sum_{r=1}^N a_r \phi_r^I(\xi) + (\omega^2 + \kappa) \sum_{r=1}^N a_r \phi_r(\xi) \end{aligned} \quad (14)$$

where

$$\phi_r^j(\xi) = d^j(\phi_r(\xi))/d\xi^j \quad (15)$$

Specifying the inner product (projection) between the error and the coordinate function must equal zero, we obtain in a matrix form

$$[A][\alpha] + u^2[B][\alpha] + 2\sqrt{\beta}u\omega[C][\alpha] + \omega^2[D][\alpha] = 0 \quad (16)$$

where

$$\begin{aligned} A &= \{a_{sr}\} = \int_0^1 \phi_r^{IV} \phi_s d\xi \\ B &= \{b_{sr}\} = \int_0^1 \phi_r^{II} \phi_s d\xi \\ C &= \{c_{sr}\} = \int_0^1 \phi_r^I \phi_s d\xi \\ D &= \{d_{sr}\} = \int_0^1 \phi_r \phi_s d\xi \\ \alpha &= [a_1 \ a_2 \ \dots \ a_N]^T \end{aligned} \quad (17)$$

### 3.1 Numerical results

In order to find the critical velocities of Eq.(16), the numbers of terms  $N$  used in the approximated solution Eq.(12) should be large enough to attain accurate results. In this section solutions are found up to high order approximations, but detailed analyses for two, four and ten-term approximate solution is presented below.

#### 3.1.1 Two-term approximate solution

Although it is mentioned in the previous paragraph that the number of coordinate functions in Eq.(10) should be large enough to achieve accurate results, it is instructive to show the solution process with less coordinate functions, for example two or four terms to obtain some approximate analytical results. For  $N = 2$  the Eq.(10) reads as follows

$$Y_2(\xi) = \sum_{r=1}^2 a_r \phi_r(\xi) = a_1 \phi_1(\xi) + a_2 \phi_2(\xi) \quad (18)$$

Based on the Boobnov-Galerkin procedure and using the first two natural frequencies for a cantilever beam, the matrices in Eq.(17) read as follows:

$$\begin{aligned} A &\equiv \lambda_r^2[I] = \begin{bmatrix} 12.3624 & 0 \\ 0 & 485.519 \end{bmatrix} \\ B &= \begin{bmatrix} 0.858244 & -11.7432 \\ 1.87385 & -13.2943 \end{bmatrix} \\ C &= \begin{bmatrix} 2 & -4.75946 \\ 0.759461 & 2 \end{bmatrix} \\ I &= \begin{bmatrix} 1 & 0 \\ 0 & 1 \end{bmatrix} \end{aligned} \quad (19)$$

Substituting these into Eq.(16), the non-triviality requirement for the

solution yields the following determinantal requirement

$$\begin{aligned}\Delta &= \begin{vmatrix} \delta_{11} & \delta_{12} \\ \delta_{21} & \delta_{22} \end{vmatrix} = 0, \text{ where} \\ \delta_{11} &= 12.3624 + 0.858244u^2 + 4u\sqrt{\beta}\omega + \omega^2, \\ \delta_{12} &= -11.7432u^2 - 9.51892u\sqrt{\beta}\omega, \\ \delta_{21} &= 1.87385u^2 + 1.51892u\sqrt{\beta}\omega, \\ \delta_{22} &= 485.519 - 13.2943u^2 + 4u\sqrt{\beta}\omega + \omega^2,\end{aligned}\tag{20}$$

which yields the following equation:

$$\begin{aligned}\omega^4 + 8u\beta^{1/2}\omega^3 - 12.436u^2\omega^2 + 497.881\omega^2 \\ + (1991.52 - 14.07u^2)u\beta^{1/2}\omega + 10.5954u^4 \\ + 252.345u^2 + 6002.16 = 0\end{aligned}\tag{21}$$

The next step is to solve previous equation for  $u$  in order to find the roots at which the system loses stability by flutter. Based on the Routh-Hurwitz stability criterion determinant previous equation can be transformed into the following Routh-Hurwitz determinant

$$\begin{aligned}T_4 &= \begin{bmatrix} t_{11} & 1 & & \\ t_{21} & t_{22} & t_{23} & 1 \\ & t_{32} & t_{33} & t_{34} \\ & & & t_{44} \end{bmatrix}, \text{ where} \\ t_{11} &= t_{23} = 8u\sqrt{\beta} \\ t_{21} &= t_{33} = 1991.5u\sqrt{\beta} - 14.07u^3\sqrt{\beta} \\ t_{22} &= t_{34} = 497.8 - 12.4u^2 + 30.4u^2\beta \\ t_{32} &= t_{44} = 6002.1 + 252.3u^2 + 10.6u^4\end{aligned}\tag{22}$$

yielding the following polynomial equation of the tenth order

$$\begin{aligned} & 2.14999 \times 10^{10} u^2 \beta - 3.82257 \times 10^8 u^4 \beta - 1.29768 \times 10^7 u^6 \beta - \\ & - 2.13825 \times 10^6 u^8 \beta + 5549.17 u^{10} \beta + 2.91267 \times 10^9 u^4 \beta^2 + \\ & + 1.01878 \times 10^8 u^6 \beta^2 + 4.27648 \times 10^6 u^8 \beta^2 - 36325.4 u^{10} \beta^2 = 0 \end{aligned} \quad (23)$$

Varying parameter  $\beta$  from 0 to 1, and solving for  $u$  we get the 10 roots of the polynomial. The smallest real positive root gives the critical velocity. For example if  $\beta = 0.1$  the ten roots of Eq.(23) are

$$\begin{aligned} u_1 &= -20.2495 \\ u_2 &= -4.22471 \\ u_3 &= -2.43852 - i4.22547 \\ u_4 &= -2.43852 + i4.22547 \\ u_5 \equiv u_6 &= 0 \\ u_7 &= 2.43852 - i4.22547 \\ u_8 &= 2.43852 + i4.22547 \\ u_9 &= 4.22471 \\ u_{10} &= 20.2495 \end{aligned} \quad (24)$$

From Eq.(24) we conclude that the non-dimensional critical velocity of the fluid at which the cantilever beam loses dynamic stability by flutter is  $u_9 = 4.22471$  when  $\beta=0.1$ . This procedure is repeated for the entire  $\beta$  interval from 0 to 1 yielding the following 100 values for the critical velocities within the two-term approximate method. Figure 2 depicts the 1000 critical velocities for the entire range of parameter  $\beta$ , and the values are presented in the embedded table.

### 3.1.2 Four-term approximate solution

To obtain a better approximate solution more terms are need in Eq.(10). In this case  $N = 4$  yields the following coordinate function

$$Y_4(\xi) = \sum_{r=1}^4 a_r \phi_r(\xi) = a_1 \phi_1(\xi) + a_2 \phi_2(\xi) + a_3 \phi_3(\xi) + a_4 \phi_4(\xi) \quad (25)$$

Based again on the Boobnov-Galerkin procedure and using the first four natural frequencies of a cantilever beam, the matrices in Eq.(17) becomes

$$\begin{aligned} A \equiv \lambda_r^2[I] &= \begin{bmatrix} 12.3624 & 0 & 0 & 0 \\ 0 & 485.519 & 0 & 0 \\ 0 & 0 & 3806.55 & 0 \\ 0 & 0 & 0 & 14617.3 \end{bmatrix} \\ B &= \begin{bmatrix} 0.858244 & -11.7432 & 27.4531 & -37.3903 \\ 1.87385 & -13.2943 & -9.04222 & 30.4012 \\ 1.56451 & 3.22933 & -45.9042 & -8.33537 \\ 1.08737 & 5.54064 & 4.25361 & -98.9182 \end{bmatrix} \\ C &= \begin{bmatrix} 2 & -4.75946 & 3.78434 & -4.11981 \\ 0.75946 & 2 & -6.22219 & 3.38338 \\ 0.215663 & 2.22219 & 2 & -8.1684 \\ 0.11981 & 0.616624 & 4.1684 & 2 \end{bmatrix} \\ I &= \begin{bmatrix} 1 & 0 & 0 & 0 \\ 0 & 1 & 0 & 0 \\ 0 & 0 & 1 & 0 \\ 0 & 0 & 0 & 1 \end{bmatrix} \end{aligned} \quad (26)$$

Substituting into Eq.(16), the non-trivial solution yields vanishing of determinant of the following matrix

$$\begin{bmatrix} \Delta_{11} & \Delta_{12} \\ \Delta_{21} & \Delta_{22} \end{bmatrix}, \quad \text{where} \quad (27)$$

$$\Delta_{11} = \begin{bmatrix} 12.3 + 0.9u^2 + 4.0u\sqrt{\beta}\omega + \omega^2 & -11.7u^2 - 9.6u\sqrt{\beta}\omega \\ 1.9u^2 + 1.5u\sqrt{\beta}\omega & 485.5 - 13.3u^2 + 4u\sqrt{\beta}\omega + \omega^2 \end{bmatrix},$$

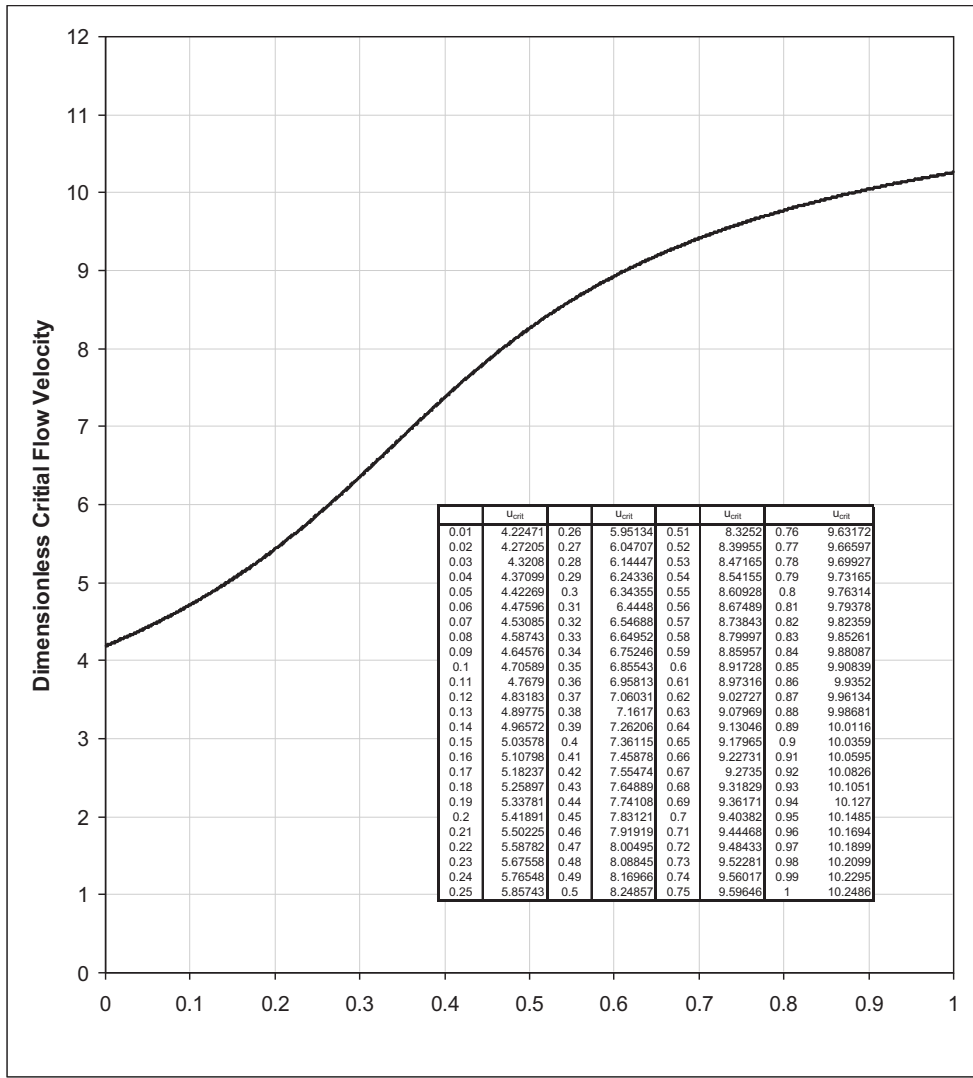


Figure 2: Non-dimensional critical fluid velocity vs.  $\beta$  within the two-term approximate solution

$$\Delta_{12} = \begin{bmatrix} 27.5u^2 + 7.6u\sqrt{\beta}\omega & -37.4u^2 - 8.2u\sqrt{\beta}\omega \\ -9.0u^2 - 12.4u\sqrt{\beta}\omega & 30.4u^2 + 6.8u\sqrt{\beta}\omega \end{bmatrix},$$

$$\Delta_{21} = \begin{bmatrix} 1.6u^2 + 0.4u\sqrt{\beta}\omega & 3.2u^2 + 4.4u\sqrt{\beta}\omega \\ 1.1u^2 + 0.2u\sqrt{\beta}\omega & 5.5u^2 + 1.2u\sqrt{\beta}\omega \end{bmatrix},$$

$$\Delta_{22} = \begin{bmatrix} 3807 - 45.9u^2 + 4u\sqrt{\beta}\omega + \omega^2 & -8.3u^2 - 16.3u\sqrt{\beta}\omega \\ 4.3u^2 8.3u\sqrt{\beta}\omega & 14620 - 98.9u^2 + 4u\sqrt{\beta}\omega + \omega^2 \end{bmatrix}.$$

Thus, we get the following polynomial equation of eighth order with respect to  $\omega$ .

$$\begin{aligned}
& 3.3397 \times 10^{11} + 7.75337 \times 10^9 u^2 + 1.2034 \times 10^8 u^4 - 952705 u^6 \\
& + 40316.8 u^8 + 1.11253 \times 10^{11} u\sqrt{\beta}\omega - 2.97707 \times 10^9 u^3\sqrt{\beta}\omega \\
& + 3.46004 \times 10^7 u^5\sqrt{\beta}\omega - 59806.8 u^7\sqrt{\beta}\omega + 2.78134 \times 10^{10} \omega^2 \\
& - 1.20972 \times 10^9 u^2\omega^2 + 1.4774 \times 10^7 u^4\omega^2 - 51414 u^6\omega^2 \\
& + 1.83251 \times 10^9 u^2\beta\omega^2 - 2.31699 \times 10^7 u^4\beta\omega^2 + 125777 u^6\beta\omega^2 \\
& + 5.18562 \times 10^8 u\sqrt{\beta}\omega^3 - 9.45285 \times 10^6 u^3\sqrt{\beta}\omega^3 + 41763.6 u^5\sqrt{\beta}\omega^3 \\
& + 6.84709 \times 10^6 u^3\sqrt{\beta^3}\omega^3 - 20570.4 u^5\sqrt{\beta^3}\omega^3 + 6.48202 \times 10^7 \omega^4 \\
& - 1.3485 \times 10^6 u^2\omega^4 + 6246.3 u^4\omega^4 + 1.97886 \times 10^6 u^2\beta\omega^4 \\
& - 12126.8 u^4\beta\omega^4 + 8838.47 u^4\beta^2\omega^4 + 227060 u\sqrt{\beta}\omega^5 - 1712.82 u^3\sqrt{\beta}\omega^5 \\
& + 2340.12 u^3\sqrt{\beta^3}\omega^5 + 18921.7 \omega^6 - 157.258 u^2\omega^6 + 292.327 u^2\beta\omega^6 \\
& + 16 u\sqrt{\beta}\omega^7 + \omega^8 = 0
\end{aligned} \tag{28}$$

From previous equation the Routh-Hurwitz determinant  $T_8$  is constructed and the following polynomial equation of 36<sup>th</sup> order is obtained, and shown in the appendix section 7.2

The reader may notice that the implementation of the Routh-Hurwitz method allows to reduce the numbers of unknowns from three in Eq.(28) to two unknowns only,  $u$  and  $\beta$ . The procedure to obtain the critical velocity from the 36<sup>th</sup> order polynomial equation is the same as used to solve Eq.(23) except this case the equation has 36 roots. For  $\beta = 0.1$

the roots read:

$$\begin{aligned}
 u_1 &= -56.1518, & u_2 &= -12.0889 - i1.10668, \\
 u_3 &= -12.0889 + i1.10668, & u_4 &= -11.8371, \\
 u_5 &= -10.5032 - i5.85159, & u_6 &= -10.5032 + i5.85159, \\
 u_7 &= -8.6922 - i0.70115, & u_8 &= -8.6922 + i0.70115, \\
 u_9 &= -7.55111 - i4.28362, & u_{10} &= -7.55111 + i4.28362, \\
 u_{11} &= -7.47838 - i3.14676, & u_{12} &= -7.47838 + i3.14676, \\
 \\ 
 u_{13} &= -4.75146, & u_{14} &= -2.3804 - i5.70271, \\
 u_{15} &= -2.3804 + i5.70271, & u_{16} &= 0, \\
 u_{17} &= 0, & u_{18} &= 0, \\
 u_{19} &= 0, & u_{20} &= 0 - i22.0263, \\
 u_{21} &= 0 + i22.0263, & u_{22} &= 2.3804 - i5.70271, \\
 u_{23} &= 2.3804 + i5.70271, & u_{24} &= 4.75146, \\
 \\ 
 u_{25} &= 7.47838 - i3.14676, & u_{26} &= 7.47838 + i3.14676, \\
 u_{27} &= 7.55111 - i4.28362, & u_{28} &= 7.55111 + i4.28362, \\
 u_{29} &= 8.6922 - i0.70115, & u_{30} &= 8.6922 + i0.70115, \\
 u_{31} &= 10.5032 - i5.85159, & u_{32} &= 10.5032 + i5.85159, \\
 u_{33} &= 11.8371, & u_{34} &= 12.0889 - i1.10668, \\
 u_{35} &= 12.0889 + i1.10668, & u_{36} &= 56.1518. 
 \end{aligned} \tag{29}$$

The first positive real root equals  $u_{24} = 4.75146$ , when  $\beta = 0.1$ .

The 100 dimensionless critical velocities for four-term approximate solution are given in Table 5, shown in the appendix, and the 1000 critical velocities are depicted in Figure 3.

With exception to Fig.1 all of the dynamic stability diagrams were constructed based on *calculated* critical velocities from their corresponding polynomial equations; no interpolated values were used in the construction of such curves.

Figure 3 shows the critical velocity stability curve is not continuous one. Two jumps are present, one in the vicinity of  $\beta = 0.3$ , and the other one in the vicinity of  $\beta = 0.7$ . These jumps are not identified in Fig.1 obtained by Gregory and Païdoussis (1966); remarkably in the same range of non-dimensional parameter  $\beta$  more than one value is depicted. A detailed analysis at each jump is considered below in order to clarify the stability contents of the pipe in these regions.

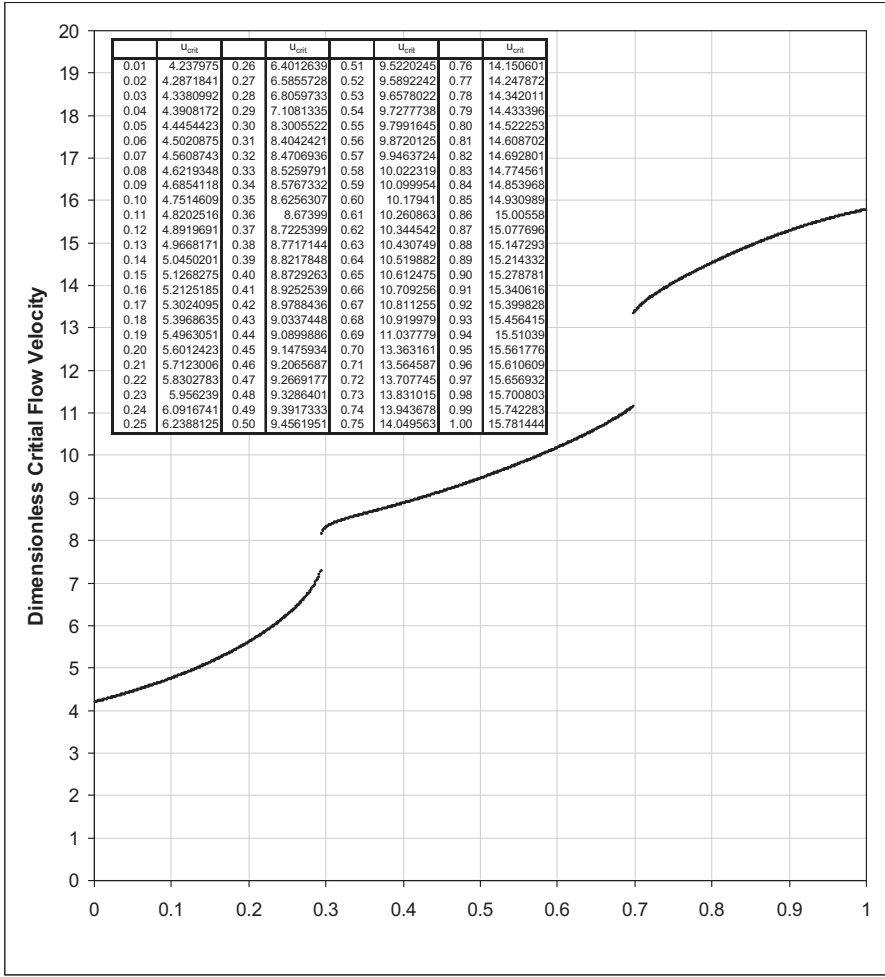
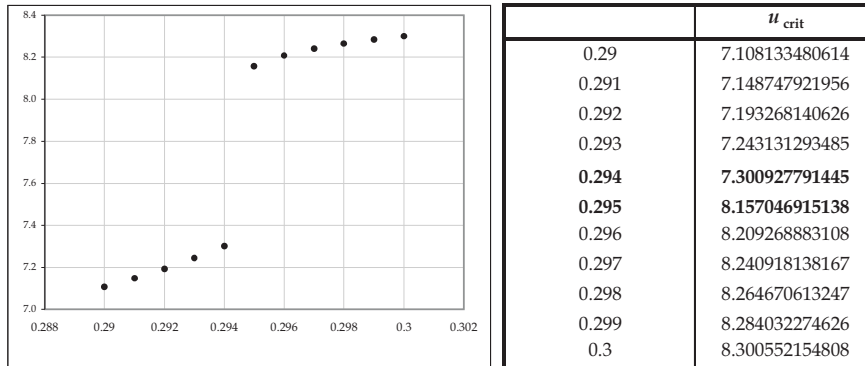
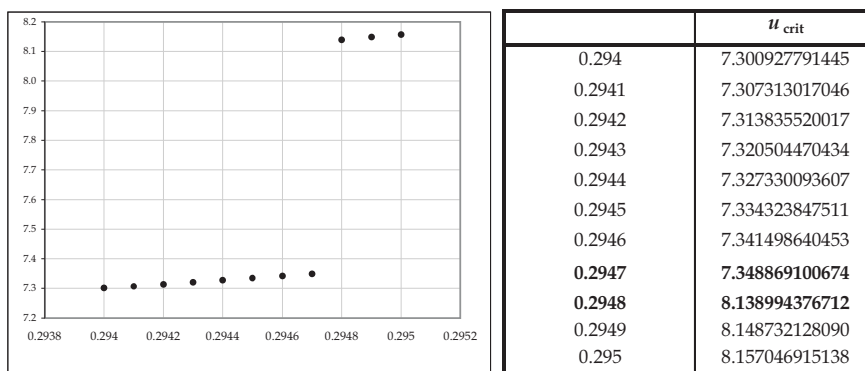


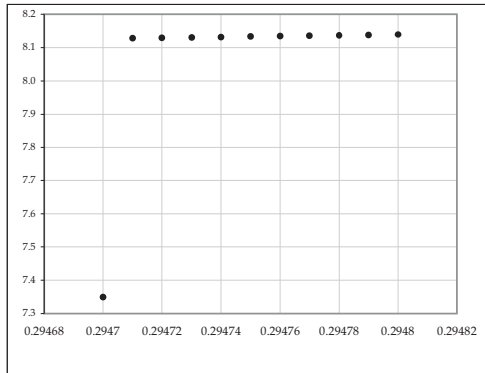
Figure 3: Non-dimensional critical fluid velocity vs. $\beta$  within the four-term approximate solution

For example, from Figure 3 the non-dimensional velocity reads 7.10813, and 8.3005 when  $\beta$  equals 0.29, and 0.3 respectively. A zoom-in process is conducted below in order to identify the behavior of the critical velocity within this range.

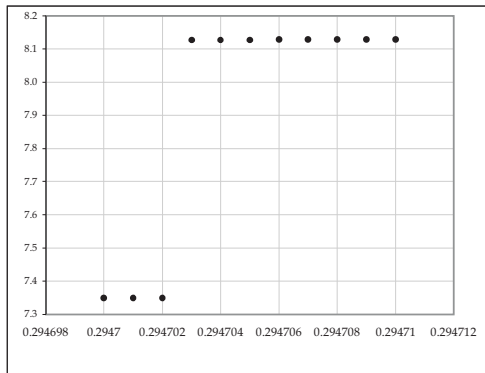
From previous graphs and tables it is possible to identify that the critical flow velocity jumps from 7.3490 when  $\beta$  equals to 0.2947026566457, to 8.1273 for  $\beta$  0.2947026566458.

The same procedure was conducted in the vicinity of  $\beta = 0.69$  show-

Figure 4: Critical flow velocity jump within  $0.290 \leq \beta \leq 0.300$ Figure 5: Critical flow velocity jump within  $0.294 \leq \beta \leq 0.295$

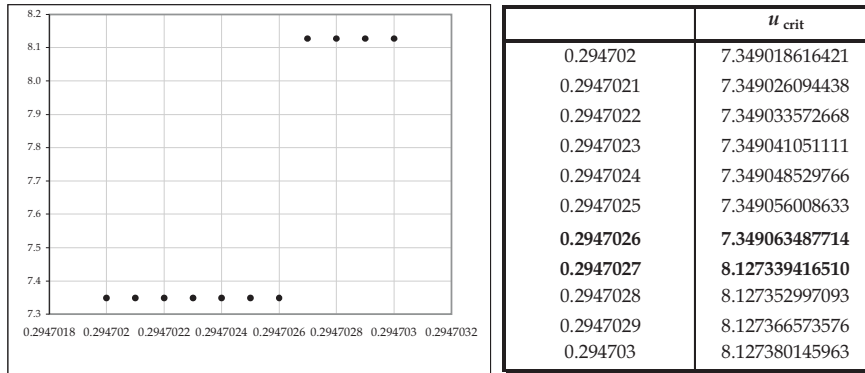
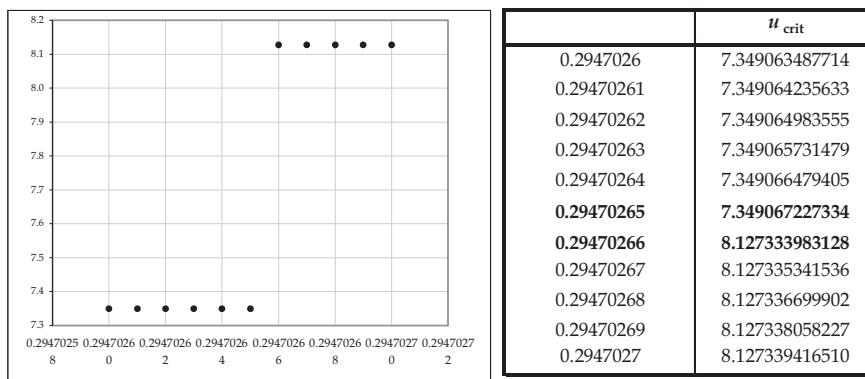


	$u_{\text{crit}}$
0.2947	7.348869100674
0.29471	8.128320222009
0.29472	8.129630466909
0.29473	8.130904701543
0.29474	8.132145398385
0.29475	8.133354762277
0.29476	8.134534769221
0.29477	8.135687198219
0.29478	8.136813657649
0.29479	8.137915607272
0.2948	8.138994376713

Figure 6: Critical flow velocity jump within  $0.294 \leq \beta \leq 0.295$ 

	$u_{\text{crit}}$
0.2947	7.348869100674
0.294701	7.348943847931
<b>0.294702</b>	<b>7.349018616421</b>
<b>0.294703</b>	<b>8.127380145963</b>
0.294704	8.127515645230
0.294705	8.127650738378
0.294706	8.127785428581
0.294707	8.127919718973
0.294708	8.128053612645
0.294709	8.128187112652
0.29471	8.128320222009

Figure 7: Critical flow velocity jump within  $0.29470 \leq \beta \leq 0.29471$

Figure 8: Critical flow velocity jump within  $0.2947026 \leq \beta \leq 0.2947027$ Figure 9: Critical flow velocity jump within  $0.29470265 \leq \beta \leq 0.29470266$

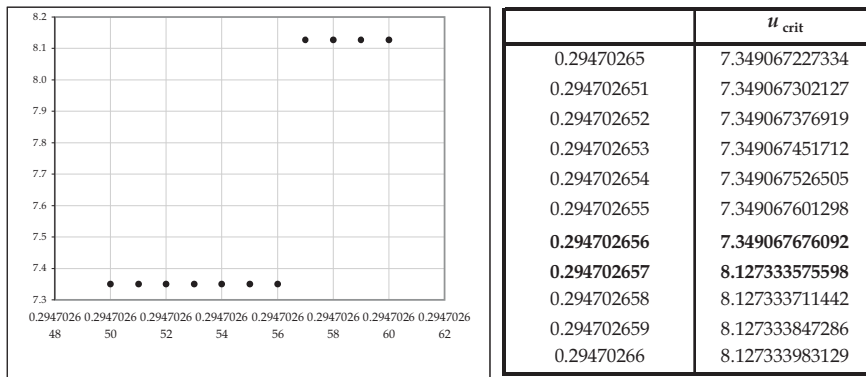


Figure 10: Critical flow velocity jump within  $0.294702656 \leq \beta \leq 0.294702657$

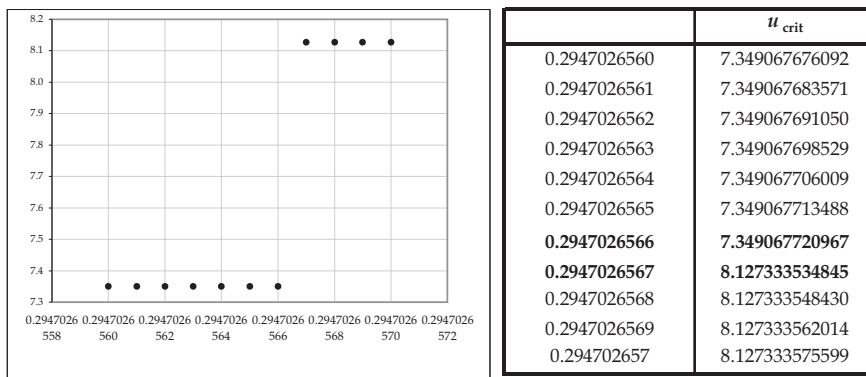


Figure 11: Critical flow velocity jump within  $0.2947026566 \leq \beta \leq 0.2947026567$

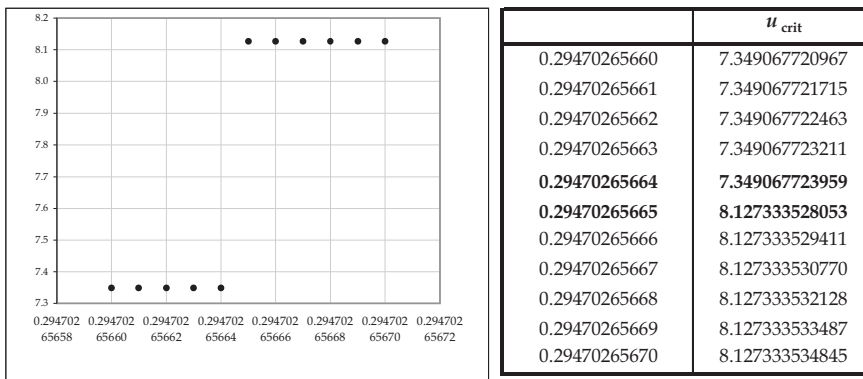


Figure 12: Critical flow velocity jump within  $0.29470265664 \leq \beta \leq 0.29470265665$

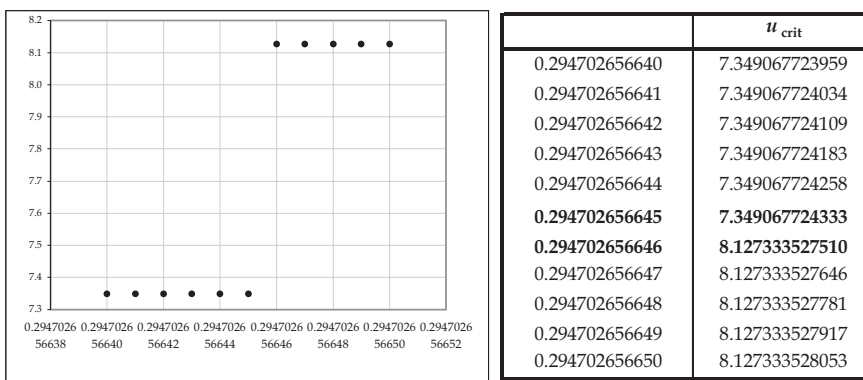


Figure 13: Critical flow velocity jump within  $0.294702656645 \leq \beta \leq 0.294702656646$

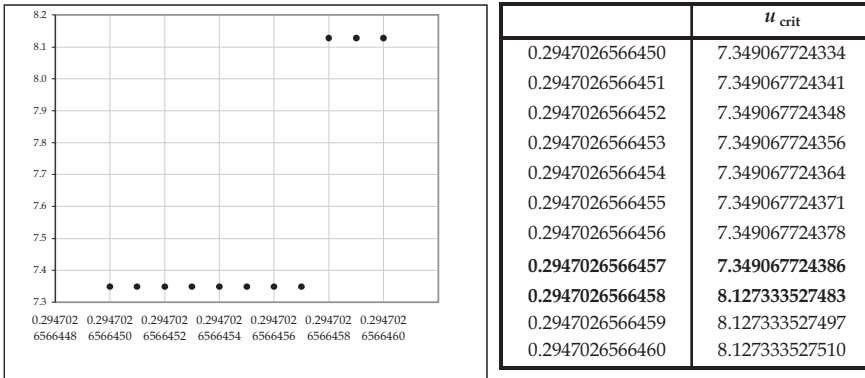


Figure 14: Critical flow velocity jump within  $0.2947026566457 \leq \beta \leq 0.2947026566458$

ing in this case the critical flow velocity experience a jump from 11.1460 when  $\beta = 0.6983611422$  to 13.3100 for  $\beta = 0.6983611423$ .

We can preliminarily conclude that increasing the number of terms in Eq.(10) from two to four show that the critical velocity is not continuous in the vicinity of  $\beta = 0.3$  and  $\beta = 0.69$ . Furthermore, these are the same ranges where Fig.1 shows the paradox of multiple velocities for a single parameter  $\beta$ . We anticipate that a third non-monotonic region shown in Gregory and Païdoussis graph will appear as another jump with in the same range when the number of approximate terms is larger than four. In this context, a ten-term approximate solution is discussed next.

### 3.1.3 Ten-term approximate solution

In order to obtain a 10-term approximate solution,  $N = 10$  should be specified in Eq.(10) along with solving Eq.(12) for the first 10 natural frequencies. Once that is done Eq.(16) can explicitly be written by substituting the values of  $\lambda_r^4$  [ $I$ ], [ $B$ ], and [ $C$ ] matrices. Numerical results for  $\lambda_r^4$  [ $I$ ], [ $B$ ], and [ $C$ ] are presented below:

$$[B] = [B_1 \ B_2 \ \dots \ B_{10}], \quad \text{where}$$

$\lambda_1^4 = 12.36236$	$\lambda_6^4 = 89135.40507$
$\lambda_2^4 = 485.51882$	$\lambda_7^4 = 173881.31566$
$\lambda_3^4 = 3806.54627$	$\lambda_8^4 = 308208.45209$
$\lambda_4^4 = 14617.27331$	$\lambda_9^4 = 508481.54327$
$\lambda_5^4 = 39943.83178$	$\lambda_{10}^4 = 793403.13454$

$$B_1 = \begin{bmatrix} 0.858244 \\ 1.87385 \\ 1.55451 \\ 1.08737 \\ 0.914043 \\ 0.740388 \\ 0.547753 \\ 0.558489 \\ 0.502 \\ 0.447733 \end{bmatrix}, \quad B_2 = \begin{bmatrix} -11.7432 \\ -13.2973 \\ 3.22933 \\ 5.54054 \\ 3.71542 \\ 3.98359 \\ 3.13977 \\ 3.10493 \\ 2.52848 \\ 2.54303 \end{bmatrix}, \quad B_3 = \begin{bmatrix} 27.4531 \\ -9.04222 \\ -45.9042 \\ 4.25361 \\ 11.2325 \\ 6.46003 \\ 8.73235 \\ 6.28643 \\ 7.14354 \\ 5.69962 \end{bmatrix},$$

$$B_4 = \begin{bmatrix} -37.3903 \\ 30.4012 \\ -8.33537 \\ -98.9182 \\ 4.735 \\ 17.1031 \\ 8.47331 \\ 13.9939 \\ 9.10852 \\ 11.8411 \end{bmatrix}, \quad B_5 = \begin{bmatrix} 51.9566 \\ -33.7091 \\ 36.3866 \\ -7.82895 \\ -171.585 \\ 5.03902 \\ 23.1335 \\ 9.9792 \\ 19.5746 \\ 11.5145 \end{bmatrix}, \quad B_6 = \begin{bmatrix} -62.8686 \\ 53.9755 \\ -31.2604 \\ 42.2345 \\ -7.52743 \\ -263.998 \\ 5.24321 \\ 29.241 \\ 11.1258 \\ 25.3422 \end{bmatrix},$$

$$B_7 = \begin{bmatrix} 76.8232 \\ -59.4185 \\ 59.0191 \\ -29.2245 \\ 48.2664 \\ -7.32316 \\ -376.15 \\ 5.39014 \\ 35.3953 \\ 12.021 \end{bmatrix}, \quad B_8 = \begin{bmatrix} -88.1833 \\ 78.2296 \\ -56.5667 \\ 64.258 \\ -27.72 \\ 54.3737 \\ -7.17623 \\ -508.041 \\ 5.50084 \\ 41.5799 \end{bmatrix}, \quad B_9 = \begin{bmatrix} 101.81 \\ -85.0626 \\ 82.563 \\ -53.722 \\ 69.8401 \\ -26.5733 \\ 60.528 \\ -7.06553 \\ -659.672 \\ 5.5872 \end{bmatrix},$$

$$B_{10} = \begin{bmatrix} -113.427 \\ 102.8 \\ -82.2862 \\ 87.238 \\ -51.3175 \\ 75.6077 \\ -25.6781 \\ 66.7126 \\ -6.97917 \\ -831.042 \end{bmatrix}.$$

By the same type of notation we have

$$[C] = [C_1 \ C_2 \ \dots \ C_{10}], \quad \text{where}$$

$$C_1 = \begin{bmatrix} 2 \\ 0.759461 \\ 0.215663 \\ 0.11981 \\ 0.0591532 \\ 0.0476684 \\ 0.0334455 \\ 0.0254946 \\ 0.0196262 \\ 0.158519 \end{bmatrix}, \quad C_2 = \begin{bmatrix} -4.75946 \\ 2 \\ 2.22219 \\ 0.616624 \\ 0.495644 \\ 0.27924 \\ 0.223159 \\ 0.152699 \\ 0.127543 \\ 0.0965614 \end{bmatrix}, \quad C_3 = \begin{bmatrix} 3.78434 \\ -6.22219 \\ 2 \\ 4.1684 \\ 0.943538 \\ 1.04193 \\ 0.515553 \\ 0.500111 \\ 0.318529 \\ 0.297682 \end{bmatrix},$$

$$\begin{aligned}
C_4 &= \begin{bmatrix} -4.11981 \\ 3.38338 \\ -8.1684 \\ 2 \\ 6.1249 \\ 1.15294 \\ 1.63332 \\ 0.715325 \\ 0.816661 \\ 0.478046 \end{bmatrix}, \quad C_5 = \begin{bmatrix} 3.93085 \\ -4.49564 \\ 3.05646 \\ -10.1249 \\ 2 \\ 8.10001 \\ 1.296 \\ 2.25 \\ 0.875676 \\ 1.15714 \end{bmatrix}, \quad C_6 = \begin{bmatrix} -4.04767 \\ 3.72508 \\ -5.04193 \\ 2.84706 \\ -12.1 \\ 2 \\ 10.0833 \\ 1.39884 \\ 2.88095 \\ 1.00415 \end{bmatrix}, \\
C_7 &= \begin{bmatrix} 3.96655 \\ -4.22316 \\ 3.48445 \\ -5.63332 \\ 2.704 \\ -14.833 \\ 2 \\ 12.0714 \\ 1.47598 \\ 3.52083 \end{bmatrix}, \quad C_8 = \begin{bmatrix} -4.02549 \\ 3.8473 \\ -4.50011 \\ 3.28468 \\ -5.25 \\ 2.60116 \\ -16.0714 \\ 2 \\ 14.0625 \\ 1.53584 \end{bmatrix}, \quad C_9 = \begin{bmatrix} 3.98037 \\ -4.12754 \\ 3.68147 \\ -4.81666 \\ 3.12432 \\ -6.88095 \\ 2.52402 \\ -18.0625 \\ 2 \\ 16.0556 \end{bmatrix}, \\
C_{10} &= \begin{bmatrix} -4.01585 \\ 3.90344 \\ -4.29768 \\ 3.52195 \\ -5.15714 \\ 2.99585 \\ -7.52083 \\ 2.46416 \\ -20.0556 \\ 2 \end{bmatrix}.
\end{aligned}$$

**Table 1.** Numerical results for  $\lambda_r^4$ ,  $[B]$  and  $[C]$  respectively.

Substituting these numerical results into Eq.(16), the determinant of Eq.(16) can be found, yielding a characteristic equation in the following form:

$$\text{Det}(\text{Eq.(16)}) = f(u, \beta, \omega) = 0 \quad (30)$$

The method of solution of Eq.(30) in order to determine the critical velocities, or the velocities at which the cantilever pipe loses stability, is based on an iterative procedure different than the Routh-Hurwitz method. Eq.(30) yields polynomial equation of degree 20, which is used to build the Routh-Hurwitz determinant. This method yields a polynomial equation with over 500 roots, and the minimum real positive root for each parameter  $\beta$  will give the critical velocity. Since the solution is based on a numerical approximation, the Routh-Hurwitz criterion may become tedious to implement and solve. Therefore instead of using this method, an alternative procedure, described in the following paragraphs, was used to find the critical fluid velocities from Eq.(30). This procedure was implemented also in solving Eq.(21) and Eq.(28) as well, yielding the same results as with the Routh-Hurwitz criterion, when the latter performs well.

A value associated with  $\beta$  is chosen, varying from 0 to 1. Once these value is assigned, Eq.(30) becomes a function with only two variables  $u$  and  $\omega$ . The critical velocity  $u_{crit}$  will be found as follows. When solving the equation for  $\omega$ , at the critical level the real part of at least one of the twenty roots changes sign from negative to positive. The procedure starts by assigning a value to  $u$ , for example  $u_o$  and solving the determinant for  $\omega$ . If all the roots have real negative part, then another, greater value of  $u_o$  is selected until one of the roots changes sign in its real component. When this occurs, the latter value of  $u_o$  it is to be called the critical velocity  $u_{crit}$  for the values of  $\kappa_o$ , and  $\beta_o$  that are specified. Since it is our desire to obtain the  $u_{crit}$  with several significant digits, this procedure is repeated so as many decimal places as desired are attained. The entire process then is repeated for other values of  $\beta_o$ .

Based on the above procedure, 1000 values of the critical velocities were obtained for a cantilever beam. These velocities are listed below.

As expected, increasing the number of terms yields a more accurate stability curve. It is remarkable that not only the third jump appears in the vicinity of  $\beta = 0.85$  but also the behavior of the stability of the pipe is reported for first time since Gregory and Païdoussis (1966) (see Fig.1) when  $\beta$  assumes values grater than 0. 95.

Once again a detailed analysis of all of these regions where the stability curve is not continuous is preformed subsequently. For example

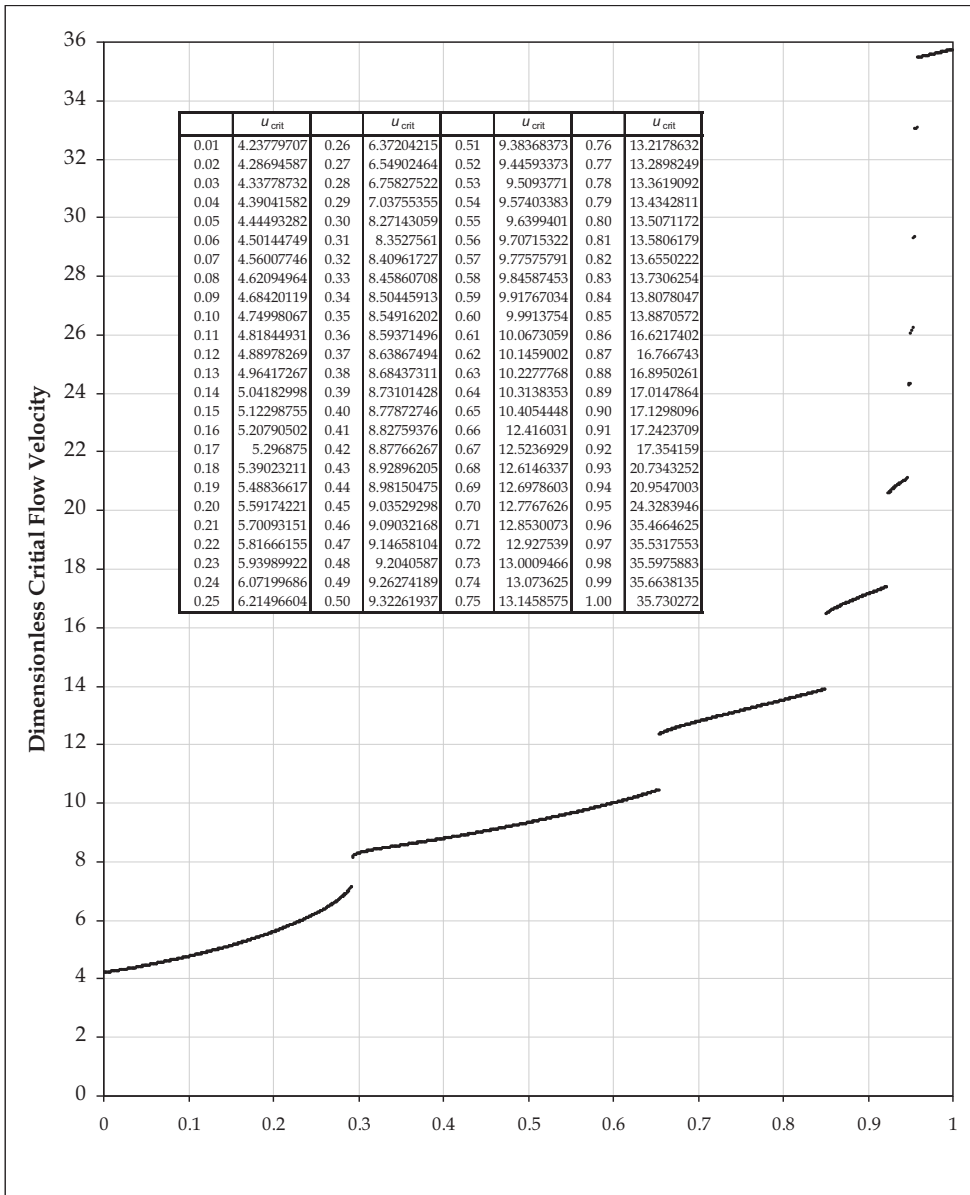


Figure 15: Critical flow velocity within ten-term approximate solution for cantilever pipe as a function of parameter  $\beta$

Figure 15 and Tables 6 to 10 reports the first jump taking place in the interval  $0.293 \leq \beta \leq 0.294$ . Zooming in between these two boundary values it allows visualizing the stability of the system. Figure 16 shows the non-dimensional critical velocity jumps from the value 7.17215 to the value 8.12215 at  $\beta = 0.2933384170$ .

The same procedure was used to analyze the jumps in the intervals  $0.654 \leq \beta \leq 0.655$ ,  $0.850 \leq \beta \leq 0.851$ ,  $0.923 \leq \beta \leq 0.924$ ,  $0.947 \leq \beta \leq 0.948$ ,  $0.950 \leq \beta \leq 0.951$ ,  $0.952 \leq \beta \leq 0.953$ ,  $0.955 \leq \beta \leq 0.956$ , and  $0.957 \leq \beta \leq 0.958$ . Results are depicted in following graphs and tables, and a summary of critical velocity jumps versus parameter  $\beta$  is shown in Table 2.

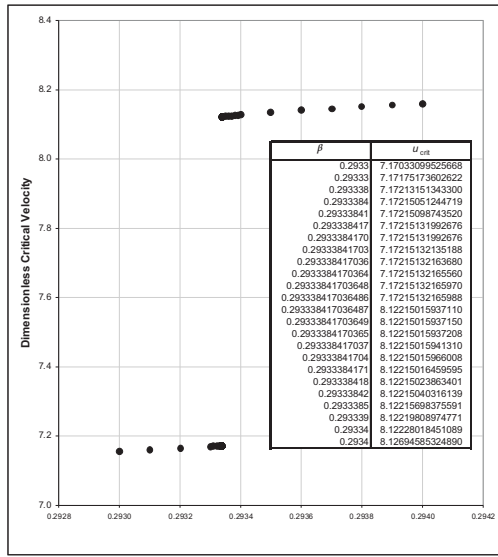
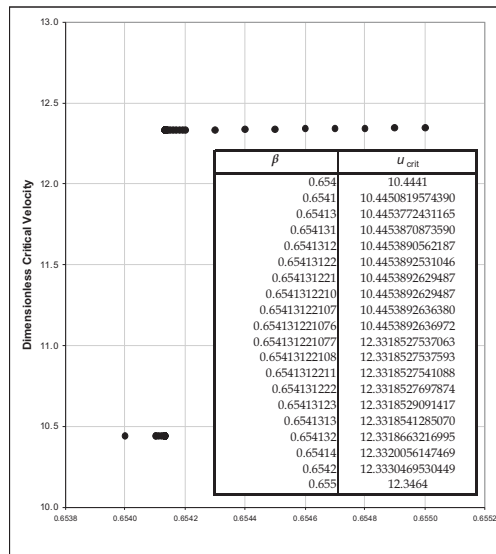
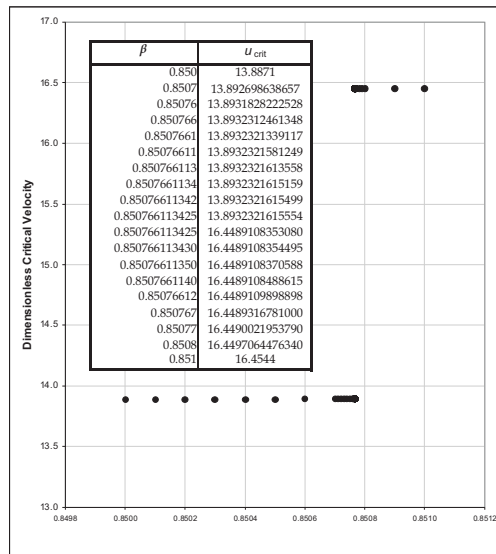


Figure 16: Critical flow velocity jump within  $0.293 \leq \beta \leq 0.294$

The following table summarizes all the critical flow velocities jumps.

Figure 17: Critical flow velocity jump within  $0.654 \leq \beta \leq 0.655$ Figure 18: Critical flow velocity jump within  $0.850 \leq \beta \leq 0.851$

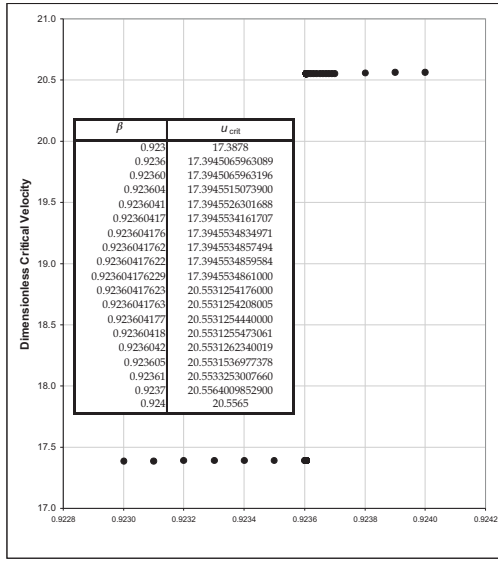


Figure 19: Critical flow velocity jump within  $0.923 \leq \beta \leq 0.924$

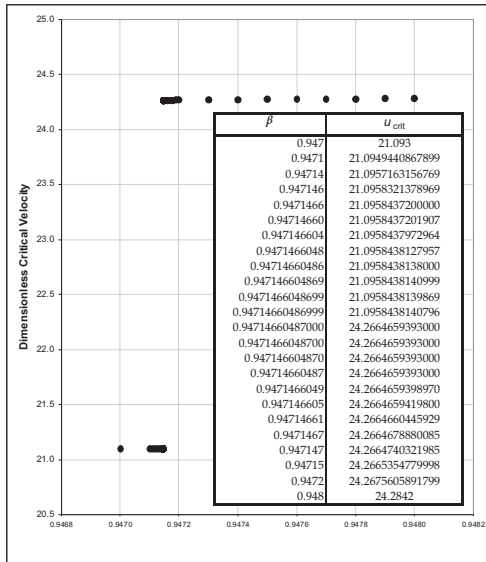
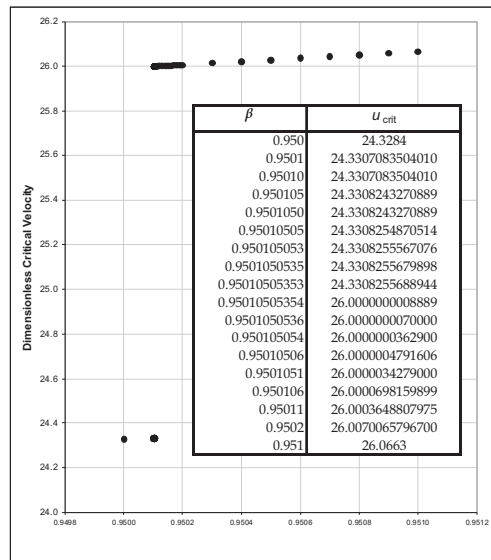
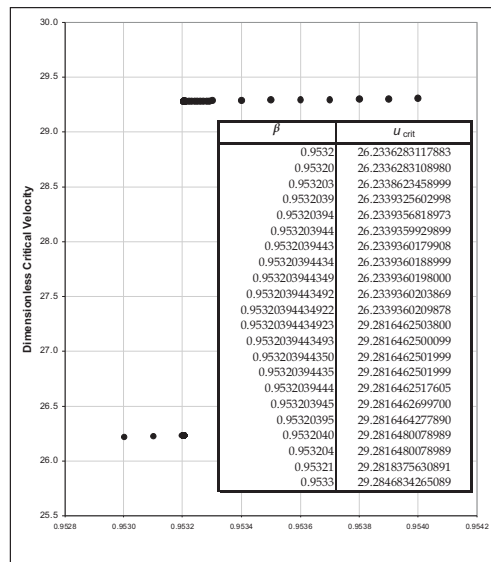
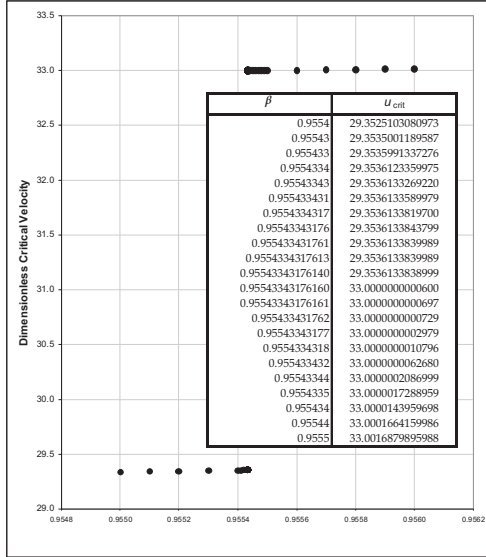
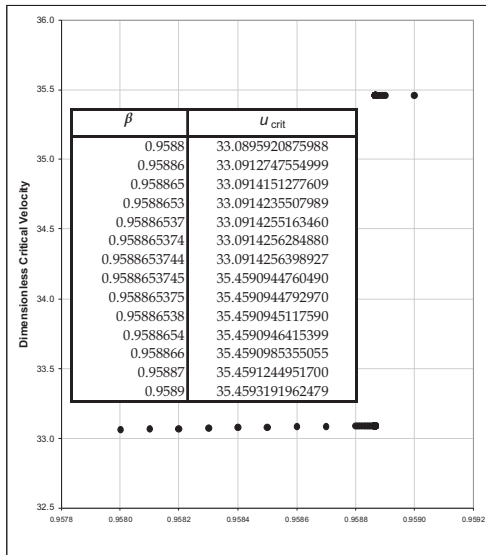


Figure 20: Critical flow velocity jump within  $0.947 \leq \beta \leq 0.948$

Figure 21: Critical flow velocity jump within  $0.950 \leq \beta \leq 0.951$ Figure 22: Critical flow velocity jump within  $0.953 \leq \beta \leq 0.954$

Figure 23: Critical flow velocity jump within  $0.955 \leq \beta \leq 0.956$ Figure 24: Critical flow velocity jump within  $0.958 \leq \beta \leq 0.959$

$\beta$		$u_{crit}$	
<b>Min</b>	<b>Max</b>	<b>Min</b>	<b>Max</b>
0.293	0.294	7.172185	8.122150
0.654	0.655	10.445389	12.331852
0.850	0.851	13.893232	16.448911
0.923	0.924	17.394553	20.553125
0.947	0.948	21.095844	24.266466
0.950	0.951	24.330826	26.000000
0.953	0.954	26.233936	29.281646
0.955	0.956	29.353613	33.000000
0.958	0.959	33.091425	35.459094

Table 2: List of the critical flow velocity jumps for entire range of parameter  $0 \leq \beta \leq 1$

## 4 Conclusion

The stability of a cantilever pipe, without elastic foundation, conveying fluid has been studied. Cantilever beam functions were used to solve the differential equations of motion. The objective was to investigate the non-monotonic behavior of the critical velocity versus the mass ratio as reported by Gregory and Païdoussis and many other authors.

In the case of pipes without elastic foundation, the stability curve indicates that critical flow velocity is monotonic for each non-dimensional parameter  $\beta$ . In other words, a unique critical velocity is obtained for each parameter  $\beta$ , showing that non-monotonic result obtained by other authors must be attributed to merely a numerical artifact. Also it suggested conducting a nonlinear analysis considering probability of a chaotic behavior of the system, with especially focusing in the regions of discontinuity.

Recently, Nikolić and Rajković [26] investigated the dynamics of fluid-conveying pipes that were simply supported at both ends via the Lyapunov-Schmidt reduction and obtained very important analytical results. It appears of much interest to conduct analogous investigation for the problem dealt with in the present study.

## Acknowledgements

Authors are grateful to Professor Michael Païdoussis for reading this paper, as well as to Dr. Isaac Lottati for his discussion of the non-monotonicity paradox. The first author also records the conversation that he had with late Professor Alexander Kornecki on the stability of pipes conveying fluid.

I. Elishakoff appreciates partial financial support provided by the J. M. Rubin Foundation of the Florida Atlantic University.

## References

- [1] Aitken J, An account of some experiments on rigidity produced by centrifugal force, *Philosophical Magazine*, Series V5, 81-105, 1878.
- [2] Becker M, Hauger W, and Winzen W, Exact Stability Analysis of Uniform Cantilever Pipes Conveying Fluid or Gas, *Archiwum Mechaniki Stosowanej*, 30, 6, 757-768, Warszawa, Poland, 1978.
- [3] Benjamin T B, Dynamics of a System of Articulated Pipes Conveying Fluid. I-Theory, *Proceedings of the Royal Society of London. Series A, Mathematical and Physical Series*, Vol. 261, Issue 1307 (May 23, 1961), 457-486.
- [4] Benjamin T B, Dynamics of a System of Articulated Pipes Conveying Fluid. II-Experiments, *Proceedings of the Royal Society of London. Series A, Mathematical and Physical Series*, Vol. 261, Issue 1307 (May 23, 1961), 487-499.
- [5] Blevins R D, Vibrations of a Pipe Containing a Fluid Flow, in *Flow Induced Vibration*, Van Norstrand Reinhold Co., pp. 287-312, 1970 (first ed.), 1977 (second ed.).
- [6] Bourrières F J, Sur un phénomène d'oscillation auto-entretenue en mécanique des fluids reels, *Publications Scientifiques et Techniques du Ministère de l'Air*, No 147, 1939.

- [7] Chen S S, Pipes Conveying Fluid, in *Flow-Induced Vibration of Circular Cylindrical Structures*, Hemisphere Publishing Corporation, pp. 141-176, 1987.
- [8] Djondjorov P A, On the Critical Velocities of Pipes on Variable Elastic Foundations, *Journal of Theoretical and Applied Mechanics*, Vol. 31 No. 4 pp. 73-81, Sofia, Bulgaria, 2001.
- [9] Djondjorov P, Vassilev V, and Dhupanov V, Dynamic Stability of Fluid Conveying Cantilevered Pipes on Elastic Foundation, *Journal of Sound and vibration*, 2001, Vol. 247(3), 537-546.
- [10] Dubin D, *Numerical and Analytical Methods for Scientists and Engineers using Mathematica<sup>®</sup>*, Wiley –Interscience, 2003.
- [11] Duncan W J, Galerkin's Method in Mechanics and Differential Equations, *Reports and Memoranda N° 1798*, August 1937.
- [12] Elishakoff I., and Impollonia N, Does a Partial Elastic Foundation Increase the Flutter Velocity of a Pipe Conveying Fluid?, *Journal of Applied Mechanics*, Vol. 68, March 2001.
- [13] Elishakoff I, and Lee L H N, On Equivalence of the Galerkin and Fourier Series Methods for One Class of Problems, *Journal of Sound and Vibrations*, Vol. 109, pp. 174-177, 1986.
- [14] Elishakoff I, Lin Y K, and Zhu L P, *Probabilistic and Convex Problem of Acoustically Excited Structures*, Elsevier, Amsterdam, The Netherlands, VIII, pp. 96, 1992.
- [15] Elishakoff I, and Zingales M, Coincidence of Boobnob-Galerkin and Closed-Form solutions in a Applied Mechanics Problem, *Journal of Applied Mechanics*, Vol. 70, pp. 777-779, 2003.
- [16] Granot D, and Kornecki A, *Static and Dynamic Instability of a Tube conveying Fluid*, Rescard Report, Technion-Israel Institute of Technology, Agricultural Engineering Faculty, Haifa, November 1973.
- [17] Gregory R W, and Païdoussis M P, Unstable Oscillation of Tubular Cantilevers Conveying Fluid. I-Theory, *Proceedings of the Royal*

- Society of London. Series A, Mathematical and Physical Series*, Vol. 293, Issue 1435 (Aug. 23, 1966), 512-527.
- [18] Gregory R W, and Païdoussis M P, Unstable Oscillation of Tubular Cantilevers Conveying Fluid. II-Experiments, *Proceedings of the Royal Society of London. Series A, Mathematical and Physical Series*, Vol. 293, Issue 1435 (Aug. 23, 1966), 528-542.
  - [19] Hurwitz A, *On the Conditions Under Which an Equation has only Roots with negative Real Parts*, *Mathematische Annalen*, Vol. 46, 1895, pp. 273-284.
  - [20] Inman D, Bending Vibration of a Beam, in *Engineering Vibration, Second Edition*, Prentice Hall, New Jersey, 2000.
  - [21] James M L, Smith G M, Wolford J C, and Whaley P W, *Vibration of Mechanical And Structural Systems: With Microcomputer Applications*, Harper & Row Publishers, 1994.
  - [22] Koiter W T, Elastic Stability, *Z, Flugwiss Weltraumforsch*, Vol. 9, pp. 205-210, 1985.
  - [23] Koiter W T, Unrealistic Follower Forces, *Journal of Sound Vibrations*, Vol. 194 No. 4, pp. 636-638, 1996.
  - [24] Long R H Jr, Experimental and Theoretical Study of Transverse Vibration of a Tube Containing Flowing Fluid, *Journal of Applied Mechanics*, Vol. 22, pp. 65-68, 1955.
  - [25] Lottati I, and Kornecki A, The Effect of an Elastic foundation and of Dissipative Forces on the Stability of Fluid-Conveying Pipes, *Journal of Sound and Vibration*, 1986, Vol. 109(2), pp. 327-338.
  - [26] Nikolic M, and Rajkovic M, Bifurcations in Nonlinear models of fluid conveying pipes fixed at both ends, *Journal of Fluids and Structures*, 2006, 22 (2), pp. 173-195.
  - [27] Niordson F I N, Vibrations of a Cylindrical Tube Containing Flowing Fluid, *Kungl. Tekniska Högskolans Handligar (Transactions of the Royal Institute of Technology)*, Stockholm, Sweden, 1953.

- [28] Öry H, Die Variationsrechnung. Der Gerade Biegebalken: Der Freitragende Traeger (Duncan), *Institut fuer Leichtbau, Rhein.-Westf. Techn. Hochschule Aachen*, 6. 3-9. (in German), 1980.
- [29] Ogata K, Basic Control Actions and Response of Control System. Routh's Stability Criterion, in *Modern Control Engineering*, Chapter 5, Prentice hall, New Jersey, 1997.
- [30] Païdoussis M P, and Issid N T, Dynamic Stability of pipes conveying fluid, *Journal Sound and Vibration*, Vol. 33, pp 267-294, 1974.
- [31] Païdoussis M P, and Li G X, Pipes Conveying Fluid: A Model Dynamical Problem, *Journal of Fluids and Structures*, Vol. 7, pp137-204, 1993.
- [32] Païdoussis M P, Pipes Conveying Fluid: Linear Dynamics I, in *Fluid-Structure Interactions Slender Structures and Axial Flow*, Vol. 1, pp. 63-163, Academic Press, London, 1998.
- [33] Panovko Ya. G, and Gubanove S V, *Stability and Oscillations of Elastic Systems, Paradoxes and Fallacies and New Concepts*, 4<sup>th</sup> Russian ed., pp. 131-132, Nauka Publishers, Moscow, 1892. (English Translation of the first edition, Consultants Bureau, New York, 1965).
- [34] Routh E J, *Dynamics of a system of Rigid Bodies*, Macmillan, NY, 1892.
- [35] Smith T E, and Herrmann G, Stability of a Beam on an Elastic Foundation subjected to a Follower force, *ASME Journal of Applied Mechanics*, Vol 39. pp. 628-629, 1972.
- [36] Tang Yu, Numerical Evaluation of Uniform Beam Modes, *Journal of Engineering Mechanics*, 2003.
- [37] Weaver W Jr, Timoshenko S P, and Young, *Vibration Problems in engineering*, Wiley, New York, 1990, pp. 363-510, Ch.5, *Continua with Infinite Degrees of Freedom*.
- [38] Wolfram S, Mathematica<sup>®</sup> 5 for Students, *Wolfram Research Inc.*, 2003.

### Appendix A.1 Transcendental equation, natural frequencies, and mode shapes for a cantilever beam

As mentioned in section 4, the natural frequencies for a cantilever beam are found by solving the following differential equation

$$\frac{d^4Y(x)}{dx^4} - \alpha^4 \frac{dY(x)}{dx} = 0, \quad \alpha = \frac{\rho A \omega^2}{EI}, \quad (\text{A.1})$$

where an exact solution in the form

$$Y(x) = \sum_j C_j e^{\lambda_j x} \quad (\text{A.2})$$

was sought. The exact solution  $Y(x)$  can also be written in the following form

$$Y(x) = \sum_{j=1}^4 C_j K_j(\lambda x) \quad (\text{A.3})$$

where  $K_j(\lambda x)$  are the Kriloff functions (see Elishakoff, Lin, Zhu, 1992).

$$\begin{aligned} K_1(\lambda x) &= \frac{1}{2} [\cosh(\lambda x) + \cos(\lambda x)] \\ K_2(\lambda x) &= \frac{1}{2} [\sinh(\lambda x) + \sin(\lambda x)] \\ K_3(\lambda x) &= \frac{1}{2} [\cosh(\lambda x) - \cos(\lambda x)] \\ K_4(\lambda x) &= \frac{1}{2} [\sinh(\lambda x) - \sin(\lambda x)] \end{aligned} \quad (\text{A.4})$$

For a clamped-free boundary the boundary condition are:

$$\begin{aligned} Y(0) &= 0 \rightarrow C_1 = 0 \\ Y'(0) &= 0 \rightarrow C_2 = 0 \end{aligned} \quad (\text{A.5})$$

At the clamped end  $x = 0$ ,  
and at the free end  $x = L$ ,

$$\begin{aligned} Y''(L) &= 0 \\ Y'''(L) &= 0 \end{aligned} \rightarrow \left\{ \begin{array}{l} \frac{1}{2} \{ [\lambda^2 \cosh(\lambda L) + \lambda^2 \cos(\lambda x)] C_3 \\ \quad + [\lambda^2 \sinh(\lambda L) + \lambda^2 \sin(\lambda L)] C_4 \} = 0 \\ \frac{1}{2} \{ [\lambda^3 \sinh(\lambda L) - \lambda^3 \sin(\lambda L)] C_3 \\ \quad + [\lambda^3 \cosh(\lambda L) + \lambda^3 \cos(\lambda L)] C_4 \} = 0 \end{array} \right. \quad (\text{A.6})$$

A non-trivial solution is to be found solving previous system for  $C_j$  such that  $C_1^2 + C_2^2 + C_3^2 + C_4^2 \neq 0$ ; this leads to the requirement that the determinant

$$\begin{vmatrix} \frac{1}{2} [\lambda^2 \cosh(\lambda L) + \lambda^2 \cos(\lambda L)] & \frac{1}{2} [\lambda^2 \sinh(\lambda L) + \lambda^2 \sin(\lambda L)] \\ \frac{1}{2} [\lambda^3 \sinh(\lambda L) - \lambda^3 \sin(\lambda L)] & \frac{1}{2} [\lambda^3 \cosh(\lambda L) + \lambda^3 \cos(\lambda L)] \end{vmatrix} = 0 \quad (\text{A.7})$$

must be zero. The transcendental equation reads

$$\cos(\lambda_n L) \cosh(\lambda_n L) = -1 \quad (\text{A.8})$$

where  $\lambda_n$  is the  $n$ -th eigenvalue of the cantilever beam. They can be found by solving Eq.(A.8). The first twenty natural frequencies are presented in the following table and graph. These frequencies were calculated with 150 significant decimal digits are shown below

From the second equation of the equation system (A.6),  $C_4$  is obtained

$$C_4 = \frac{\sin(\lambda) - \sinh(\lambda)}{\cos(\lambda) + \cosh(\lambda)} C_3 \quad (\text{A.9})$$

Substituting it into first equation of (A.6), the mode shape function for a cantilever beam becomes

$$\begin{aligned} \phi_n(x) = & \cosh(\lambda_n x) - \cos(\lambda_n x) \\ & + \frac{\sin(\lambda_n L) - \sinh(\lambda_n L)}{\cos(\lambda_n L) + \cosh(\lambda_n L)} [\sinh(\lambda_n x) - \sin(\lambda_n x)] \end{aligned}$$

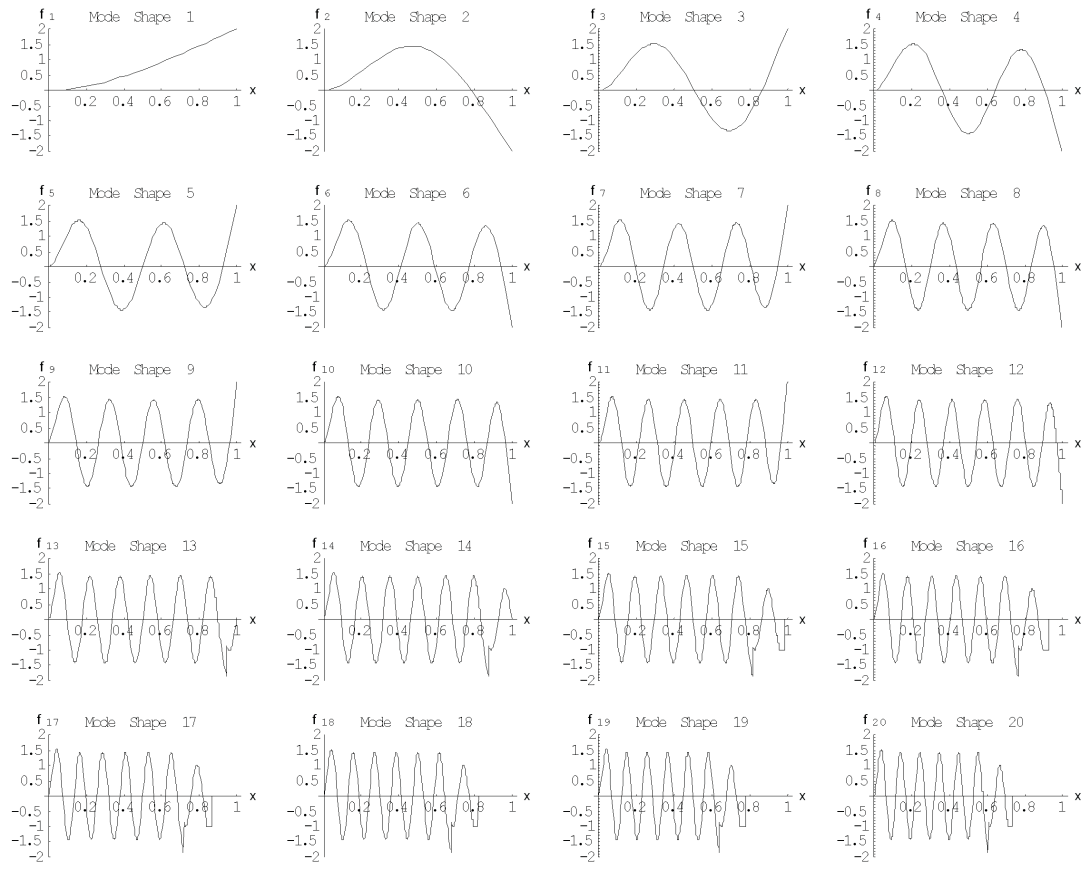


Figure 25: First twenty mode shapes of a cantilever beam

Eigenvalue number, $n$	Eigenvalue $\lambda_j L$
$\lambda_1$	1.875104068711961166445308241078214162570111733 53106998824541371310567995284042863852656655058 18860370841046452209626292398393082335974076132 96206514729095377678279
$\lambda_2$	4.694091132974174576436391778019812049389896737 54576682897280327784907793680105250800358850278 15542731577257033967642034266556337181057329119 84881121194060906960892
$\lambda_3$	7.854757438237612564861008582764570457848541929 23004669442328144882656142140865352823498667893 99980053621315469238896572902413320877863470138 540829653650049511299684
$\lambda_4$	10.99554073487546699066734910785470293961297277 46515868875057287685326879028776766558537942814 00174238143686049701057447983408873263025813955 6972848694427186233322063
$\lambda_5$	14.13716839104647058091704681255177206860307679 29746625766039022106086281379699731755372051449 04034641567581964582523158084873381280291005838 1902738264076069344243391
$\lambda_6$	17.27875953208823633354392841437582208593451963 55502051801958340982051718276595050623839718037 43635844503296459883041471802164171019022782567 2670636043472804833520526
$\lambda_7$	20.42035225104125099441581194794783704613728889 45442214697100775769321846422746174259960570627 78479255749297670347583624235788389368762059250 575352873269546572972228
$\lambda_8$	23.56194490180644350152025324019807551703126599 00508917589510782463168368287878017403473290318 53498003662515955863646712939802634663453774917 224834829646296570235033
$\lambda_9$	26.7035375551829880544547873808817400922749669 14435209202107214771578591731170518784640870678 23896036931209749374615067180321732166179712220 6399687226824425687960277
$\lambda_{10}$	29.84513020910281726378873090743040506336991605 02374036319155608470136070236506604192284746071 98766662773561419927942509846360911900571751734 0426161532219120696734086

Table 3: First ten eigenvalues of a cantilever beam

Eigenvalue number, $n$	Eigenvalue $\lambda_j L$
$\lambda_{11}$	32.98672286269283844616831418385368300036703604 16460549808087764493052572295275774425061196469 50881769231766440840439609320136258641117444993 6725758447729223044526068
$\lambda_{12}$	36.12831551628262183428116220464844632308953935 25020607930504027174619834098778687675128808090 18419240199005749277541908144406280989389413631 8205689088244759829372863
$\lambda_{13}$	39.26990816987241549841601651429208343003023484 15151413241300324716486025312869664536627388816 09842092935049195200716879464555283363769217569 9345363083838518506510908
$\lambda_{14}$	42.41150082346220871848369576744047332913756616 53338112675555213837974788339602636122502102035 07482566481864357230800765800637259982224752059 3757975488507543494776216
$\lambda_{15}$	45.55309347705200195774125762710448454623614335 92748201834344967475087936589320466770408679307 19576360388047613774295349724905903914254180710 438231634771757903762298
$\lambda_{16}$	48.69468613064179519616954946831914491598792714 77220708533544167246642274814132301577051134863 23444958283725730203819136066053929812272879256 8856155883040163982228718
$\lambda_{17}$	51.83627878423158843463367731632967243882096610 37235959422610118032437519984444837563043118715 75570324003278709894376013793188372409993686044 6548359173529087634063954
$\lambda_{18}$	54.97787143782138167309625655007162337162633235 05072072200995105589358098462212986510310859507 2532806191371482328444577050005944494466357846 1179810211502391944596259
$\lambda_{19}$	58.11946409141117491155890270550399868463952918 40733570597141388446827615068951910054379611885 69176072252430680071568823166696236675829907564 5260827925070850726169304
$\lambda_{20}$	61.26105674500096815002154596898791392501638205 76586479248407973946844533790891850728063174529 55158996401205958843973377262741839421231091841 8026490655072712373879582

Table 4: Eigenvalues  $\lambda_{11}, \lambda_{12}, \dots, \lambda_{20}$  of a cantilever beam

## Appendix A.2 Polynomial equation of 36<sup>th</sup> order

$$\begin{aligned}
 & (1.51299 \cdot 10^{58} - 1.76238 \cdot 10^{57}u^2 - 7.58977 \cdot 10^{55}u^4 - 1.89972 \cdot 10^{54}u^6 \\
 & 4.24838 \cdot 10^{52}u^8 - 1.27757 \cdot 10^{51}u^{10} - 3.94457 \cdot 10^{49}u^{12} - 9.31428 \cdot 10^{47}u^{14} \\
 & 1.59303 \cdot 10^{46}u^{16} - 1.98656 \cdot 10^{44}u^{18} - 1.81435 \cdot 10^{42}u^{20} - 1.20417 \cdot 10^{40}u^{22} \\
 & 5.6707 \cdot 10^{37}u^{24} - 1.80566 \cdot 10^{35}u^{26} - 3.54831 \cdot 10^{32}u^{28} - 3.5824 \cdot 10^{29}u^{30} \\
 & 1.26609 \cdot 10^{26}u^{32})u^{4-2} - (3.35628 \cdot 10^{57} - 2.776581 \cdot 10^{56}u^2 - 9.69319 \cdot 10^{54}u^4 \\
 & 2.14333 \cdot 10^{53}u^6 - 5.12935 \cdot 10^{51}u^8 - 1.67209 \cdot 10^{50}u^{10} - 4.8622 \cdot 10^{48}u^{12} \\
 & 1.0272 \cdot 10^{47}u^{14} - 1.55386 \cdot 10^{45}u^{16} - 1.70015 \cdot 10^{43}u^{18} - 1.34515 \cdot 10^{41}u^{20} \\
 & 7.57743 \cdot 10^{38}u^{22} - 2.9297 \cdot 10^{36}u^{24} - 7.2087 \cdot 10^{33}u^{26} - 9.51917 \cdot 10^{30}u^{28} \\
 & 4.14136 \cdot 10^{27}u^{30})u^{6-3} - (2.41411 \cdot 10^{56} - 1.6682 \cdot 10^{55}u^2 - 4.84653 \cdot 10^{53}u^4 \\
 & 9.59202 \cdot 10^{51}u^6 - 2.55957 \cdot 10^{50}u^8 - 8.8777 \cdot 10^{48}u^{10} - 2.39629 \cdot 10^{47}u^{12} \\
 & 4.49608 \cdot 10^{45}u^{14} - 5.92495 \cdot 10^{43}u^{16} - 5.52861 \cdot 10^{41}u^{18} - 3.61013 \cdot 10^{39}u^{20} \\
 & 1.59125 \cdot 10^{37}u^{22} - 4.40429 \cdot 10^{34}u^{24} - 6.57237 \cdot 10^{31}u^{26} - 3.6061 \cdot 10^{28}u^{28})u^{8-4} \\
 & (9.15099 \cdot 10^{54} - 5.16291 \cdot 10^{53}u^2 - 1.22668 \cdot 10^{52}u^4 - 2.23155 \cdot 10^{50}u^6 \\
 & 7.10389 \cdot 10^{48}u^8 - 2.5145 \cdot 10^{47}u^{10} - 6.12045 \cdot 10^{45}u^{12} - 9.97375 \cdot 10^{43}u^{14} \\
 & 1.11225 \cdot 10^{42}u^{16} - 8.47412 \cdot 10^{39}u^{18} - 4.27094 \cdot 10^{37}u^{20} - 1.32659 \cdot 10^{35}u^{22} \\
 & 2.18058 \cdot 10^{32}u^{24} - 1.31504 \cdot 10^{29}u^{26})u^{10-5} - (1.9744 \cdot 10^{53} - 8.78746 \cdot 10^{51}u^2 \\
 & 1.63147 \cdot 10^{50}u^4 - 2.93936 \cdot 10^{48}u^6 - 1.19018 \cdot 10^{47}u^8 - 4.03431 \cdot 10^{45}u^{10} \\
 & 8.52887 \cdot 10^{43}u^{12} - 1.1689 \cdot 10^{42}u^{14} - 1.05899 \cdot 10^{40}u^{16} - 6.19355 \cdot 10^{37}u^{18} \\
 & 2.19551 \cdot 10^{35}u^{20} - 4.07556 \cdot 10^{32}u^{22} - 2.80781 \cdot 10^{29}u^{24})u^{12-6} \\
 & (2.30715 \cdot 10^{51} - 7.60092 \cdot 10^{49}u^2 - 1.0149 \cdot 10^{48}u^4 - 2.23401 \cdot 10^{46}u^6 \\
 & 1.12933 \cdot 10^{45}u^8 - 3.40092 \cdot 10^{43}u^{10} - 5.98136 \cdot 10^{41}u^{12} - 6.61258 \cdot 10^{39}u^{14} \\
 & 4.54213 \cdot 10^{37}u^{16} - 1.84154 \cdot 10^{35}u^{18} - 3.83663 \cdot 10^{32}u^{20} - 2.96811 \cdot 10^{29}u^{22})u^{14-7} \\
 & (1.20287 \cdot 10^{49} - 2.28179 \cdot 10^{47}u^2 - 2.18452 \cdot 10^{45}u^4 - 8.63383 \cdot 10^{43}u^6 \\
 & 4.68766 \cdot 10^{42}u^8 - 1.12362 \cdot 10^{41}u^{10} - 1.57145 \cdot 10^{39}u^{12} - 1.29329 \cdot 10^{37}u^{14} \\
 & 6.05307 \cdot 10^{40}u^{16} - 1.41337 \cdot 10^{32}u^{18} - 1.21187 \cdot 10^{29}u^{20})u^{16-8} - 0
 \end{aligned}$$

$\beta$	$u_{\text{crit}}$	$\beta$	$u_{\text{crit}}$	$\beta$	$u_{\text{crit}}$	$\beta$	$u_{\text{crit}}$
0.01	4.237975	0.26	6.4012639	0.51	9.5220245	0.76	14.150601
0.02	4.2871841	0.27	6.5855728	0.52	9.5892242	0.77	14.247872
0.03	4.3380992	0.28	6.8059733	0.53	9.6578022	0.78	14.342011
0.04	4.3908172	0.29	7.1081335	0.54	9.7277738	0.79	14.433396
0.05	4.4454423	0.30	8.3005522	0.55	9.7991645	0.80	14.522253
0.06	4.5020875	0.31	8.4042421	0.56	9.8720125	0.81	14.608702
0.07	4.5608743	0.32	8.4706936	0.57	9.9463724	0.82	14.692801
0.08	4.6219348	0.33	8.5259791	0.58	10.022319	0.83	14.774561
0.09	4.6854118	0.34	8.5767332	0.59	10.099954	0.84	14.853968
0.10	4.7514609	0.35	8.6256307	0.60	10.17941	0.85	14.930989
0.11	4.8202516	0.36	8.67399	0.61	10.260863	0.86	15.00558
0.12	4.8919691	0.37	8.7225399	0.62	10.344542	0.87	15.077696
0.13	4.9668171	0.38	8.7717144	0.63	10.430749	0.88	15.147293
0.14	5.0450201	0.39	8.8217848	0.64	10.519882	0.89	15.214332
0.15	5.1268275	0.40	8.8729263	0.65	10.612475	0.90	15.278781
0.16	5.2125185	0.41	8.9252539	0.66	10.709256	0.91	15.340616
0.17	5.3024095	0.42	8.9788436	0.67	10.811255	0.92	15.399828
0.18	5.3968635	0.43	9.0337448	0.68	10.919979	0.93	15.456415
0.19	5.4963051	0.44	9.0899886	0.69	11.037779	0.94	15.51039
0.20	5.6012423	0.45	9.1475934	0.70	13.363161	0.95	15.561776
0.21	5.7123006	0.46	9.2065687	0.71	13.564587	0.96	15.610609
0.22	5.8302783	0.47	9.2669177	0.72	13.707745	0.97	15.656932
0.23	5.956239	0.48	9.3286401	0.73	13.831015	0.98	15.700803
0.24	6.0916741	0.49	9.3917333	0.74	13.943678	0.99	15.742283
0.25	6.2388125	0.50	9.4561951	0.75	14.049563	1.00	15.781444

Table 5: Dimensionless critical velocities obtained within four-term approximate solution.

$\beta$	$u_{\text{crit}}$	$\beta$	$u_{\text{crit}}$	$\beta$	$u_{\text{crit}}$	$\beta$	$u_{\text{crit}}$
0.001	4.194938	0.051	4.450493	0.101	4.756704	0.151	5.131306
0.002	4.199637	0.052	4.456072	0.102	4.763454	0.152	5.139661
0.003	4.204353	0.053	4.461672	0.103	4.770231	0.153	5.148055
0.004	4.209083	0.054	4.467293	0.104	4.777036	0.154	5.156488
0.005	4.213830	0.055	4.472933	0.105	4.783868	0.155	5.164959
0.006	4.218592	0.056	4.478595	0.106	4.790728	0.156	5.173469
0.007	4.223369	0.057	4.484277	0.107	4.797616	0.157	5.182018
0.008	4.228163	0.058	4.489979	0.108	4.804532	0.158	5.190607
0.009	4.232972	0.059	4.495703	0.109	4.811477	0.159	5.199236
0.010	4.237797	0.060	4.501447	0.110	4.818449	0.160	5.207905
0.011	4.242638	0.061	4.507213	0.111	4.825451	0.161	5.216614
0.012	4.247496	0.062	4.513000	0.112	4.832481	0.162	5.225365
0.013	4.252369	0.063	4.518809	0.113	4.839540	0.163	5.234156
0.014	4.257259	0.064	4.524639	0.114	4.846629	0.164	5.242989
0.015	4.262166	0.065	4.530490	0.115	4.853746	0.165	5.251864
0.016	4.267088	0.066	4.536364	0.116	4.860894	0.166	5.260780
0.017	4.272028	0.067	4.542259	0.117	4.868071	0.167	5.269740
0.018	4.276984	0.068	4.548176	0.118	4.875278	0.168	5.278741
0.019	4.281956	0.069	4.554116	0.119	4.882515	0.169	5.287786
0.020	4.286946	0.070	4.560077	0.120	4.889783	0.170	5.296875
0.021	4.291952	0.071	4.566062	0.121	4.897081	0.171	5.306007
0.022	4.296976	0.072	4.572068	0.122	4.904410	0.172	5.315184
0.023	4.302016	0.073	4.578098	0.123	4.911770	0.173	5.324405
0.024	4.307074	0.074	4.584150	0.124	4.919161	0.174	5.333671
0.025	4.312149	0.075	4.590225	0.125	4.926583	0.175	5.342982
0.026	4.317242	0.076	4.596323	0.126	4.934037	0.176	5.352339
0.027	4.322352	0.077	4.602445	0.127	4.941523	0.177	5.361742
0.028	4.327479	0.078	4.608589	0.128	4.949040	0.178	5.371192
0.029	4.332624	0.079	4.614758	0.129	4.956590	0.179	5.380688
0.030	4.337787	0.080	4.620950	0.130	4.964173	0.180	5.390232
0.031	4.342968	0.081	4.627165	0.131	4.971788	0.181	5.399824
0.032	4.348167	0.082	4.633405	0.132	4.979436	0.182	5.409463
0.033	4.353384	0.083	4.639669	0.133	4.987117	0.183	5.419151
0.034	4.358619	0.084	4.645957	0.134	4.994831	0.184	5.428888
0.035	4.363872	0.085	4.652269	0.135	5.002579	0.185	5.438675
0.036	4.369144	0.086	4.658606	0.136	5.010361	0.186	5.448512
0.037	4.374434	0.087	4.664967	0.137	5.018176	0.187	5.458398
0.038	4.379742	0.088	4.671354	0.138	5.026026	0.188	5.468336
0.039	4.385070	0.089	4.677765	0.139	5.033911	0.189	5.478325
0.040	4.390416	0.090	4.684201	0.140	5.041830	0.190	5.488366
0.041	4.395781	0.091	4.690663	0.141	5.049784	0.191	5.498459
0.042	4.401165	0.092	4.697150	0.142	5.057774	0.192	5.508606
0.043	4.406568	0.093	4.703663	0.143	5.065798	0.193	5.518805
0.044	4.411990	0.094	4.710201	0.144	5.073859	0.194	5.529058
0.045	4.417432	0.095	4.716765	0.145	5.081956	0.195	5.539366
0.046	4.422893	0.096	4.723356	0.146	5.090089	0.196	5.549729
0.047	4.428373	0.097	4.729972	0.147	5.098258	0.197	5.560147
0.048	4.433873	0.098	4.736615	0.148	5.106464	0.198	5.570622
0.049	4.439393	0.099	4.743284	0.149	5.114707	0.199	5.581153
0.050	4.444933	0.100	4.749981	0.150	5.122988	0.200	5.591742

Table 6: Dimensionless critical flow velocities values for  $0.001 \leq \beta \leq 0.200$

$\beta$	$u_{crit}$	$\beta$	$u_{crit}$	$\beta$	$u_{crit}$	$\beta$	$u_{crit}$
0.201	5.602389	0.251	6.229970	0.301	8.282061	0.351	8.553612
0.202	5.613094	0.252	6.245117	0.302	8.291843	0.352	8.558062
0.203	5.623859	0.253	6.260412	0.303	8.300940	0.353	8.562512
0.204	5.634684	0.254	6.275859	0.304	8.309470	0.354	8.566963
0.205	5.645569	0.255	6.291464	0.305	8.317526	0.355	8.571415
0.206	5.656516	0.256	6.307231	0.306	8.325180	0.356	8.575870
0.207	5.667525	0.257	6.323166	0.307	8.332487	0.357	8.580326
0.208	5.678596	0.258	6.339275	0.308	8.339494	0.358	8.584786
0.209	5.689732	0.259	6.355565	0.309	8.346240	0.359	8.589248
0.210	5.700932	0.260	6.372042	0.310	8.352756	0.360	8.593715
0.211	5.712196	0.261	6.388714	0.311	8.359068	0.361	8.598186
0.212	5.723527	0.262	6.405588	0.312	8.365200	0.362	8.602661
0.213	5.734925	0.263	6.422672	0.313	8.371170	0.363	8.607142
0.214	5.746391	0.264	6.439977	0.314	8.376996	0.364	8.611628
0.215	5.757925	0.265	6.457511	0.315	8.382692	0.365	8.616120
0.216	5.769529	0.266	6.475284	0.316	8.388270	0.366	8.620617
0.217	5.781204	0.267	6.493310	0.317	8.393742	0.367	8.625121
0.218	5.792950	0.268	6.511599	0.318	8.399119	0.368	8.629632
0.219	5.804769	0.269	6.530166	0.319	8.404408	0.369	8.634150
0.220	5.816662	0.270	6.549025	0.320	8.409617	0.370	8.638675
0.221	5.828629	0.271	6.568192	0.321	8.414754	0.371	8.643207
0.222	5.840672	0.272	6.587685	0.322	8.419826	0.372	8.647748
0.223	5.852792	0.273	6.607525	0.323	8.424837	0.373	8.652296
0.224	5.864991	0.274	6.627731	0.324	8.429792	0.374	8.656852
0.225	5.877269	0.275	6.648330	0.325	8.434698	0.375	8.661417
0.226	5.889628	0.276	6.669347	0.326	8.439557	0.376	8.665990
0.227	5.902069	0.277	6.690814	0.327	8.444374	0.377	8.670572
0.228	5.914593	0.278	6.712764	0.328	8.449153	0.378	8.675163
0.229	5.927203	0.279	6.735236	0.329	8.453896	0.379	8.679764
0.230	5.939899	0.280	6.758275	0.330	8.458607	0.380	8.684373
0.231	5.952683	0.281	6.781932	0.331	8.463288	0.381	8.688992
0.232	5.965557	0.282	6.806266	0.332	8.467943	0.382	8.693621
0.233	5.978523	0.283	6.831346	0.333	8.472573	0.383	8.698259
0.234	5.991581	0.284	6.857254	0.334	8.477180	0.384	8.702908
0.235	6.004735	0.285	6.884090	0.335	8.481767	0.385	8.707566
0.236	6.017985	0.286	6.911971	0.336	8.486336	0.386	8.712235
0.237	6.031335	0.287	6.941045	0.337	8.490888	0.387	8.716914
0.238	6.044785	0.288	6.971497	0.338	8.495425	0.388	8.721604
0.239	6.058338	0.289	7.003562	0.339	8.499948	0.389	8.726304
0.240	6.071997	0.290	7.037554	0.340	8.504459	0.390	8.731014
0.241	6.085763	0.291	7.073899	0.341	8.508960	0.391	8.735736
0.242	6.099640	0.292	7.113209	0.342	8.513450	0.392	8.740468
0.243	6.113630	0.293	7.156408	0.343	8.517933	0.393	8.745211
0.244	6.127735	0.294	8.159007	0.344	8.522408	0.394	8.749966
0.245	6.141959	0.295	8.191128	0.345	8.526878	0.395	8.754731
0.246	6.156304	0.296	8.213677	0.346	8.531341	0.396	8.759508
0.247	6.170774	0.297	8.231564	0.347	8.535801	0.397	8.764295
0.248	6.185372	0.298	8.246611	0.348	8.540257	0.398	8.769095
0.249	6.200101	0.299	8.259725	0.349	8.544710	0.399	8.773905
0.250	6.214966	0.300	8.271431	0.350	8.549162	0.400	8.778727

Table 7: Dimensionless critical flow velocities values for  $0.201 \leq \beta \leq 0.400$

$\beta$	$u_{\text{crit}}$	$\beta$	$u_{\text{crit}}$	$\beta$	$u_{\text{crit}}$	$\beta$	$u_{\text{crit}}$
0.401	8.783561	0.451	9.040740	0.501	9.328672	0.551	9.646601
0.402	8.788407	0.452	9.046200	0.502	9.334737	0.552	9.653276
0.403	8.793264	0.453	9.051672	0.503	9.340814	0.553	9.659964
0.404	8.798132	0.454	9.057156	0.504	9.346903	0.554	9.666664
0.405	8.803013	0.455	9.062653	0.505	9.353003	0.555	9.673379
0.406	8.807905	0.456	9.068162	0.506	9.359116	0.556	9.680106
0.407	8.812809	0.457	9.073683	0.507	9.365240	0.557	9.686848
0.408	8.817726	0.458	9.079217	0.508	9.371376	0.558	9.693602
0.409	8.822654	0.459	9.084763	0.509	9.377524	0.559	9.700371
0.410	8.827594	0.460	9.090322	0.510	9.383684	0.560	9.707153
0.411	8.832546	0.461	9.095892	0.511	9.389855	0.561	9.713949
0.412	8.837510	0.462	9.101475	0.512	9.396039	0.562	9.720760
0.413	8.842487	0.463	9.107071	0.513	9.402234	0.563	9.727584
0.414	8.847475	0.464	9.112678	0.514	9.408441	0.564	9.734422
0.415	8.852476	0.465	9.118298	0.515	9.414660	0.565	9.741275
0.416	8.857489	0.466	9.123930	0.516	9.420891	0.566	9.748142
0.417	8.862514	0.467	9.129575	0.517	9.427134	0.567	9.755024
0.418	8.867551	0.468	9.135231	0.518	9.433389	0.568	9.761920
0.419	8.872601	0.469	9.140900	0.519	9.439655	0.569	9.768832
0.420	8.877663	0.470	9.146581	0.520	9.445934	0.570	9.775758
0.421	8.882737	0.471	9.152274	0.521	9.452224	0.571	9.782699
0.422	8.887824	0.472	9.157980	0.522	9.458526	0.572	9.789656
0.423	8.892922	0.473	9.163697	0.523	9.464841	0.573	9.796628
0.424	8.898034	0.474	9.169427	0.524	9.471167	0.574	9.803615
0.425	8.903157	0.475	9.175168	0.525	9.477505	0.575	9.810618
0.426	8.908294	0.476	9.180922	0.526	9.483856	0.576	9.817637
0.427	8.913442	0.477	9.186688	0.527	9.490218	0.577	9.824672
0.428	8.918603	0.478	9.192466	0.528	9.496592	0.578	9.831723
0.429	8.923776	0.479	9.198256	0.529	9.502979	0.579	9.838790
0.430	8.928962	0.480	9.204059	0.530	9.509377	0.580	9.845875
0.431	8.934160	0.481	9.209873	0.531	9.515788	0.581	9.852975
0.432	8.939371	0.482	9.215699	0.532	9.522210	0.582	9.860093
0.433	8.944594	0.483	9.221538	0.533	9.528645	0.583	9.867228
0.434	8.949830	0.484	9.227388	0.534	9.535093	0.584	9.874380
0.435	8.955078	0.485	9.233250	0.535	9.541552	0.585	9.881550
0.436	8.960338	0.486	9.239125	0.536	9.548024	0.586	9.888737
0.437	8.965611	0.487	9.245011	0.537	9.554508	0.587	9.895943
0.438	8.970897	0.488	9.250909	0.538	9.561004	0.588	9.903167
0.439	8.976194	0.489	9.256820	0.539	9.567513	0.589	9.910409
0.440	8.981505	0.490	9.262742	0.540	9.574034	0.590	9.917670
0.441	8.986828	0.491	9.268676	0.541	9.580567	0.591	9.924950
0.442	8.992163	0.492	9.274622	0.542	9.587114	0.592	9.932250
0.443	8.997511	0.493	9.280580	0.543	9.593672	0.593	9.939569
0.444	9.002871	0.494	9.286550	0.544	9.600244	0.594	9.946908
0.445	9.008243	0.495	9.292532	0.545	9.606828	0.595	9.954267
0.446	9.013628	0.496	9.298526	0.546	9.613425	0.596	9.961646
0.447	9.019026	0.497	9.304531	0.547	9.620034	0.597	9.969047
0.448	9.024436	0.498	9.310549	0.548	9.626656	0.598	9.976468
0.449	9.029858	0.499	9.316578	0.549	9.633292	0.599	9.983911
0.450	9.035293	0.500	9.322619	0.550	9.639940	0.600	9.991375

Table 8: Dimensionless critical flow velocities values for  $0.401 \leq \beta \leq 0.600$

$\beta$	$u_{crit}$	$\beta$	$u_{crit}$	$\beta$	$u_{crit}$	$\beta$	$u_{crit}$
0.601	9.998862	0.651	10.414986	0.701	12.784487	0.751	13.153065
0.602	10.006371	0.652	10.424607	0.702	12.792187	0.752	13.160271
0.603	10.013904	0.653	10.434310	0.703	12.799863	0.753	13.167474
0.604	10.021459	0.654	10.444098	0.704	12.807516	0.754	13.174676
0.605	10.029038	0.655	12.346413	0.705	12.815147	0.755	13.181877
0.606	10.036642	0.656	12.361981	0.706	12.822757	0.756	13.189076
0.607	10.044270	0.657	12.376554	0.707	12.830348	0.757	13.196274
0.608	10.051923	0.658	12.390330	0.708	12.837919	0.758	13.203471
0.609	10.059601	0.659	12.403454	0.709	12.845472	0.759	13.210667
0.610	10.067306	0.660	12.416031	0.710	12.853007	0.760	13.217863
0.611	10.075037	0.661	12.428143	0.711	12.860526	0.761	13.225059
0.612	10.082795	0.662	12.439853	0.712	12.868028	0.762	13.232254
0.613	10.090581	0.663	12.451213	0.713	12.875515	0.763	13.239449
0.614	10.098394	0.664	12.462264	0.714	12.882987	0.764	13.246644
0.615	10.106237	0.665	12.473041	0.715	12.890445	0.765	13.253839
0.616	10.114108	0.666	12.483573	0.716	12.897889	0.766	13.261035
0.617	10.122010	0.667	12.493885	0.717	12.905320	0.767	13.268231
0.618	10.129942	0.668	12.503997	0.718	12.912738	0.768	13.275428
0.619	10.137905	0.669	12.513928	0.719	12.920144	0.769	13.282626
0.620	10.145900	0.670	12.523693	0.720	12.927539	0.770	13.289825
0.621	10.153928	0.671	12.533306	0.721	12.934923	0.771	13.297025
0.622	10.161989	0.672	12.542780	0.722	12.942296	0.772	13.304227
0.623	10.170084	0.673	12.552126	0.723	12.949659	0.773	13.311430
0.624	10.178214	0.674	12.561352	0.724	12.957012	0.774	13.318635
0.625	10.186380	0.675	12.570467	0.725	12.964355	0.775	13.325842
0.626	10.194583	0.676	12.579480	0.726	12.971690	0.776	13.333050
0.627	10.202823	0.677	12.588397	0.727	12.979016	0.777	13.340261
0.628	10.211101	0.678	12.597224	0.728	12.986334	0.778	13.347475
0.629	10.219419	0.679	12.605968	0.729	12.993644	0.779	13.354691
0.630	10.227777	0.680	12.614634	0.730	13.000947	0.780	13.361909
0.631	10.236176	0.681	12.623225	0.731	13.008242	0.781	13.369131
0.632	10.244619	0.682	12.631748	0.732	13.015530	0.782	13.376355
0.633	10.253104	0.683	12.640205	0.733	13.022812	0.783	13.383583
0.634	10.261635	0.684	12.648601	0.734	13.030088	0.784	13.390814
0.635	10.270212	0.685	12.656939	0.735	13.037357	0.785	13.398049
0.636	10.278836	0.686	12.665222	0.736	13.044621	0.786	13.405287
0.637	10.287509	0.687	12.673452	0.737	13.051880	0.787	13.412529
0.638	10.296232	0.688	12.681634	0.738	13.059133	0.788	13.419775
0.639	10.305007	0.689	12.689769	0.739	13.066381	0.789	13.427026
0.640	10.313835	0.690	12.697860	0.740	13.073625	0.790	13.434281
0.641	10.322718	0.691	12.705909	0.741	13.080864	0.791	13.441541
0.642	10.331658	0.692	12.713918	0.742	13.088099	0.792	13.448805
0.643	10.340656	0.693	12.721889	0.743	13.095331	0.793	13.456075
0.644	10.349714	0.694	12.729824	0.744	13.102558	0.794	13.463349
0.645	10.358834	0.695	12.737724	0.745	13.109782	0.795	13.470629
0.646	10.368018	0.696	12.745592	0.746	13.117003	0.796	13.477915
0.647	10.377269	0.697	12.753428	0.747	13.124221	0.797	13.485206
0.648	10.386589	0.698	12.761234	0.748	13.131436	0.798	13.492504
0.649	10.395980	0.699	12.769012	0.749	13.138648	0.799	13.499807
0.650	10.405445	0.700	12.776763	0.750	13.145858	0.800	13.507117

Table 9: Dimensionless critical flow velocities values for  $0.601 \leq \beta \leq 0.800$

$\beta$	$u_{\text{crit}}$	$\beta$	$u_{\text{crit}}$	$\beta$	$u_{\text{crit}}$	$\beta$	$u_{\text{crit}}$
0.801	13.514434	0.851	16.454360	0.901	17.141146	0.951	26.066323
0.802	13.521757	0.852	16.476648	0.902	17.152460	0.952	26.141432
0.803	13.529088	0.853	16.497576	0.903	17.163753	0.953	26.218070
0.804	13.536425	0.854	16.517416	0.904	17.175028	0.954	29.306983
0.805	13.543771	0.855	16.536363	0.905	17.186285	0.955	29.339371
0.806	13.551124	0.856	16.554560	0.906	17.197527	0.956	33.014466
0.807	13.558485	0.857	16.572119	0.907	17.208755	0.957	33.040573
0.808	13.565854	0.858	16.589124	0.908	17.219970	0.958	33.067466
0.809	13.573232	0.859	16.605646	0.909	17.231175	0.959	35.459968
0.810	13.580618	0.860	16.621740	0.910	17.242371	0.960	35.466462
0.811	13.588013	0.861	16.637455	0.911	17.253559	0.961	35.472964
0.812	13.595418	0.862	16.652828	0.912	17.264741	0.962	35.479471
0.813	13.602832	0.863	16.667895	0.913	17.275919	0.963	35.485985
0.814	13.610256	0.864	16.682682	0.914	17.287093	0.964	35.492506
0.815	13.617690	0.865	16.697215	0.915	17.298266	0.965	35.499033
0.816	13.625135	0.866	16.711516	0.916	17.309439	0.966	35.505566
0.817	13.632590	0.867	16.725604	0.917	17.320613	0.967	35.512104
0.818	13.640056	0.868	16.739494	0.918	17.331790	0.968	35.518649
0.819	13.647533	0.869	16.753203	0.919	17.342972	0.969	35.525199
0.820	13.655022	0.870	16.766743	0.920	17.354159	0.970	35.531755
0.821	13.662523	0.871	16.780127	0.921	17.365354	0.971	35.538317
0.822	13.670036	0.872	16.793364	0.922	17.376558	0.972	35.544883
0.823	13.677562	0.873	16.806466	0.923	17.387772	0.973	35.551455
0.824	13.685101	0.874	16.819440	0.924	20.566481	0.974	35.558032
0.825	13.692653	0.875	16.832296	0.925	20.598415	0.975	35.564613
0.826	13.700218	0.876	16.845039	0.926	20.628278	0.976	35.571199
0.827	13.707798	0.877	16.857678	0.927	20.656525	0.977	35.577790
0.828	13.715392	0.878	16.870218	0.928	20.683473	0.978	35.584385
0.829	13.723001	0.879	16.882666	0.929	20.709348	0.979	35.590985
0.830	13.730625	0.880	16.895026	0.930	20.734325	0.980	35.597588
0.831	13.738265	0.881	16.907304	0.931	20.758537	0.981	35.604196
0.832	13.745921	0.882	16.919504	0.932	20.782089	0.982	35.610807
0.833	13.753594	0.883	16.931631	0.933	20.805069	0.983	35.617422
0.834	13.761283	0.884	16.943689	0.934	20.827548	0.984	35.624040
0.835	13.768990	0.885	16.955682	0.935	20.849585	0.985	35.630662
0.836	13.776715	0.886	16.967613	0.936	20.871231	0.986	35.637286
0.837	13.784459	0.887	16.979486	0.937	20.892529	0.987	35.643914
0.838	13.792221	0.888	16.991304	0.938	20.913519	0.988	35.650545
0.839	13.800003	0.889	17.003070	0.939	20.934233	0.989	35.657178
0.840	13.807805	0.890	17.014786	0.940	20.954700	0.990	35.663813
0.841	13.815627	0.891	17.026457	0.941	20.974948	0.991	35.670452
0.842	13.823471	0.892	17.038084	0.942	20.994999	0.992	35.677092
0.843	13.831336	0.893	17.049670	0.943	21.014876	0.993	35.683734
0.844	13.839224	0.894	17.061217	0.944	21.034598	0.994	35.690378
0.845	13.847135	0.895	17.072727	0.945	21.054184	0.995	35.697024
0.846	13.855069	0.896	17.084204	0.946	21.073650	0.996	35.703671
0.847	13.863028	0.897	17.095648	0.947	21.093013	0.997	35.710320
0.848	13.871012	0.898	17.107063	0.948	24.284231	0.998	35.716970
0.849	13.879021	0.899	17.118449	0.949	24.305834	0.999	35.723620
0.850	13.887057	0.900	17.129810	0.950	24.328395	1.000	35.730272

Table 10: Dimensionless critical flow velocities values for  $0.801 \leq \beta \leq 1.00$

Submitted on September 2005.

## **Paradoks nemonotonosti stabilnosti cevi kroz koje protiče fluid**

UDK 534.14, 534.16, 534.21

Paradoksalni rezultat nemonotone relacije izmedju kritične brzine fluida koji protiče kroz elastičnu cev, i masenog odnosa je prvi put saopšten pre oko četiri decenije. Od tada je ovaj rezultat ponavljan u brojnim knjigama i člancima. U ovoj studiji se pomenuti paradoks ponovo analizira. Zaključuje se da je ovo numerički artifakt; umesto nemonotonosti ustvari postoje skokovi.